5-2021

Investigating the Role of Charge Separation in Triplet State Formation in Zinc Dipyrrin Photosensitizers

Irene Y. Dzaye
East Tennessee State University

Investigating the Role of Charge Separation in Triplet State Formation in Zinc Dipyrrin Photosensitizers

---

A thesis

presented to

the faculty of the Department of Chemistry

East Tennessee State University

In partial fulfillment

of the requirements for the degree

Master of Science in Chemistry

---

by

Irene Yayra Dzaye

May 2021

Dr. Catherine E. McCusker

Dr. Marina Roginskaya

Dr. Reza Mohseni

Keywords: photosensitizers, triplet excited state, reductive photochemistry, zinc dipyrrin complexes

ABSTRACT

Investigating the Role of Charge Separation in Triplet State

Formation in Zinc Dipyrrin Photosensitizers

by

Irene Yayra Dzaye

About 85% of the world's energy is derived from non-renewable sources—coal, petroleum, and natural gas. Solar photocatalysis is one way to potentially generate cheap renewable fuels by harnessing energy from the sun using a photosensitizer and converting it into chemical energy. The efficiency of a photosensitizer depends on its capacity to form a prolonged triplet excited state. Zinc dipyrrin complexes have the potential to be efficient sensitizers for reductive photochemistry, but their ability to form long-lived triplet excited states still needs extensive research. The overall aim of this research is to probe the role charge separation plays in the formation of triplet state in metal complexes of dipyrrin photosensitizers. The specific objectives are to synthesize and characterize zinc and boron dipyrrin complexes, analyze their photophysical properties—such as steady state spectroscopy, low temperature emission spectroscopy—and quantify their triplet states using time-resolved transient absorption spectroscopy.

ACKNOWLEDGEMENTS

I would like to express my sincere gratitude to my research supervisor and academic advisor, Dr. Catherine E. McCusker, for her remarkable support and direction throughout my research. I am thankful to my thesis committee members Dr. Marina Roginskaya and Dr. Reza Mohseni for their help and advice. I am very grateful.

I am grateful to ETSU Office of Research and Sponsored Programs and the American Chemical Society Petroleum Research Fund for their financial support throughout the research. I would also like to say “thank you” to the faculty and staff of the Department of Chemistry, ETSU.

Lastly, I appreciate my fiancé, my family and friends for their support, encouragements, prayers, and love shown me through my period of studies and research.

TABLE OF CONTENTS

LIST OF TABLES

LIST OF FIGURES

LIST OF ABBREVIATIONS

Abbreviation	Name
BODIPY	Boron difluoride dipyrrinato
CS	Charge-separated
CT	Charge transfer
DCM	Dichloromethane
DDQ	2,3-dichloro-5,6-dicyano 1,4-benzoquinone
ISC	Intersystem crossing
NMR	Nuclear Magnetic Resonance
PMT	Photomultiplier tube
SD	Standard deviation
TEA	Triethylamine
TFA	Trifluoroacetic acid
THF	Tetrahydrofuran
$Zn(DIPY)_2$	Bis(2, 8-diethyl-1, 3, 7, 9-tetramethyl-5-mesityldipyrrinato) zinc(II)
ZnDPY	Bis(1,3,7,9-tetramethyl-5-mesityldipyrrinato)zinc(II)
ZnIDPY	Bis(2, 8-diiodo-1, 3, 7, 9-tetramethyl-5-mesityldipyrrinato) zinc(II)

CHAPTER 1: INTRODUCTION

Background

The average temperature of the Earth's climatic system has increased exponentially, over the last century, to an alarming rate. Approximately 80% of global energy is derived from non-renewable sources such as coal, petroleum, and natural gas.[1,2] The US in 2018 accounted for 80.2% of its energy from carbon-based sources as shown in figure 1. This gives rise to two problems needing attention. There is the problem of deriving energy from non-renewable sources—hydrocarbon deposits—which are bound to run out since the fuels are not regenerated.

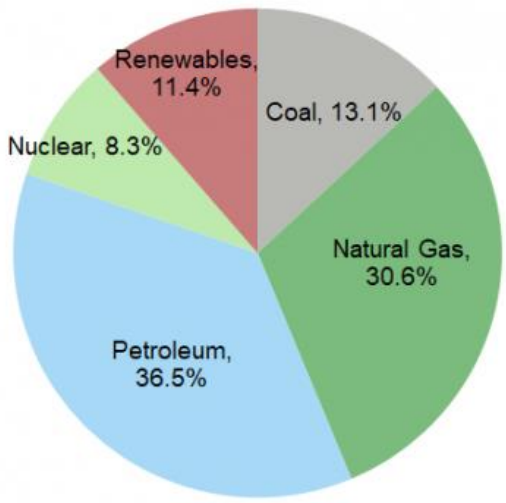

Figure 1: US energy consumption by source in 2018[3]

Another serious issue is the large accumulation of waste from the burning of fossil fuels deposited in the atmosphere. Among such waste are gas pollutants like carbon monoxide, nitrogen oxides, and carbon dioxide. Carbon dioxide, in particular, has over the decades

increased vastly in concentration in the atmosphere. It is the major greenhouse gas of much concern presently due to its contribution to global warming and the high rise of sea levels.[2,4]

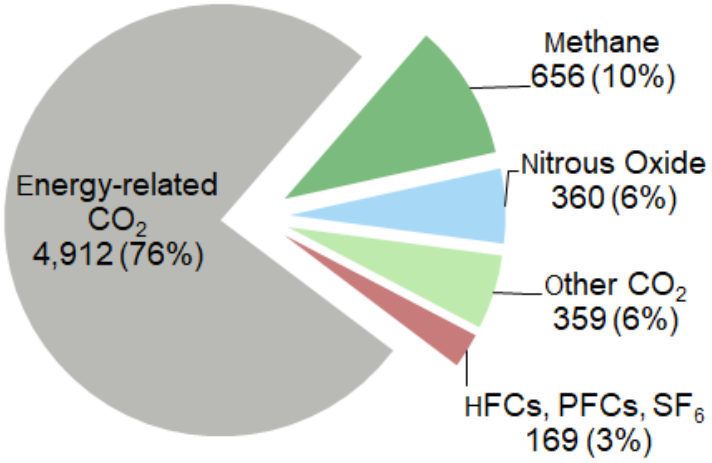

Figure 2: US greenhouse gas emissions in 2017 measured in metric tons[3]

The search for greener energy has caught the attention of most scientists with varying levels of research on the rise. This research is among many that seek to solve the problem of energy recycle and global warming by reducing the atmospheric concentration of carbon dioxide through the conversion of CO_2 into useful starting materials and energy sources.

Reductive photocatalysis of carbon dioxide presents a solution that can help solve both problems mentioned above, where carbon dioxide is converted into useful energy sources making fossil fuels renewable and reducing atmospheric concentration of CO_2. There are a number of catalysts that are available to achieve the reduction process. However, photosensitizers used with these catalysts are quite expensive and inaccessible. The goal is

therefore to produce photosensitizers incorporating first-row transition metals that are earth-abundant and cheap to be used with catalysts for the photocatalytic reduction of CO_2.

Photolysis of CO_2

Carbon dioxide is a symmetric linear molecule with a point group of $D_{\infty h}$. It has a Gibbs free energy of formation of almost –400 kJ/mol.[5] Due to its high stability, conversion of CO_2 will require a high amount of energy thermally. An excellent alternative to achieve effective fragmentation of CO_2 is photocatalysis.[6] With green chemistry being the goal, one way to attain high energy that is cheap is solar energy. Power from the sun is clean, renewable and can generate high power needed to breakdown CO_2.

Natural photosynthesis, from a long time ago, has been one process that has successfully harvested solar energy and transformed it into chemical energy for storage to be used as fuel for subsequent reactions.[7] It involves the splitting of H_2O to form H_2 and O_2 and conversion of CO_2 to carbohydrates.[2] The process occurs in three generalized pathways: light absorption by pigment molecules, electron transport to create holes, and catalysis.[8,9] Pigmented molecules such as chlorophyll (figure 3) and carotenoids in plants, bilins in cyanobacteria and algae, absorb solar energy to initiate the process, serving as nature's photosensitizers. The ability of the pigments to absorb light is due to the presence of alternating single and double bonds in their carbon chain forming a conjugated π- electron system. Upon absorption of a photon, the light-harvesting complexes transfer an electron to a nearby electron acceptor by a process termed as photoinduced charge/electron transfer.[10] This serves as the initial step for the photosynthetic process.

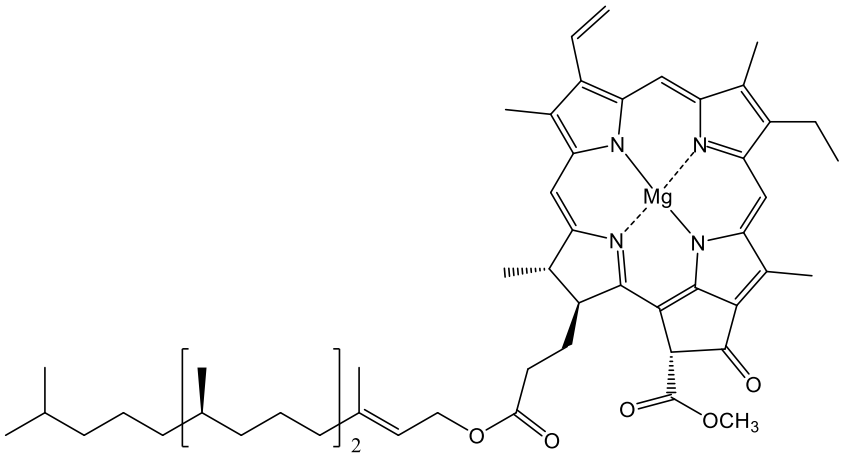

Figure 3: An example of light-harvesting compound in green plants[8]

The success story associated with nature's photosynthesis since the beginning of time has inspired scientists to create artificial photosynthetic systems for solar energy conversion.[9] There are fundamentally three components involved with setting up a photosynthetic system: a photosensitizer to harness the solar energy, an electron donor to serve as the electron source, and a catalyst to aid in the chemical conversion of CO_2 to useful fuel bases. Figure 4 presents a pictorial description of reductive photocatalysis. During the process, the photosensitizer S absorbs light from the sun resulting in an electronic excited state S^*. The excited photosensitizer accepts an electron from a sacrificial electron donor D to form S^{-}. The reduced photosensitizer then undergoes a second electron transfer to a nearby catalyst and returns to the ground state. The catalyst further carries out the reduction process.

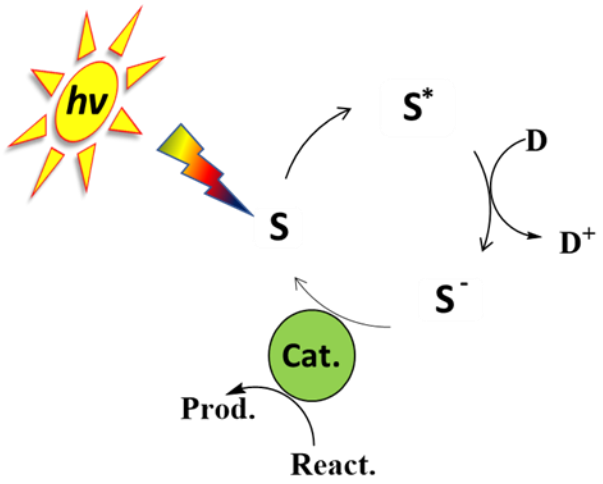

Figure 4: Reductive photocatalytic cycle[1]

In the modelling of synthetic photosensitizers, there are some key factors to consider for CO_2 reduction. The photosensitizer should primarily absorb light energy from the sun and form an electronically stable excited state with enough energy to make an excited state reaction (electron transfer) thermodynamically favorable. The light-absorbing species should have a long-excited state lifetime enough to allow reaction to compete with excited state decay. Another vital factor is that the excited sensitizer should be able to undergo the oxidation/reduction reaction for many cycles without decomposing. Carbon dioxide has a high solubility in polar solvents and therefore, its reduction is much more efficient in such media. The photosensitizer must also be soluble in the polar medium for effective reduction.[1,11] Most synthetic photosensitizers that have been employed in photochemistry are metal complexes of Ir, Ru, Os, amongst other second and third row transition metals.[12–14] Though effective, the problem with these photosensitizers is the availability and cost of the metals. Such metals are considered rare earth metals; hence, they are not readily available and expensive to acquire. In order to run the artificial photosynthetic

systems for a long time, availability and cost are of great importance. Zinc complexes offer a potential solution in the synthesis of cheap and effective photosensitizers.

Steady State Spectroscopy of Complexes

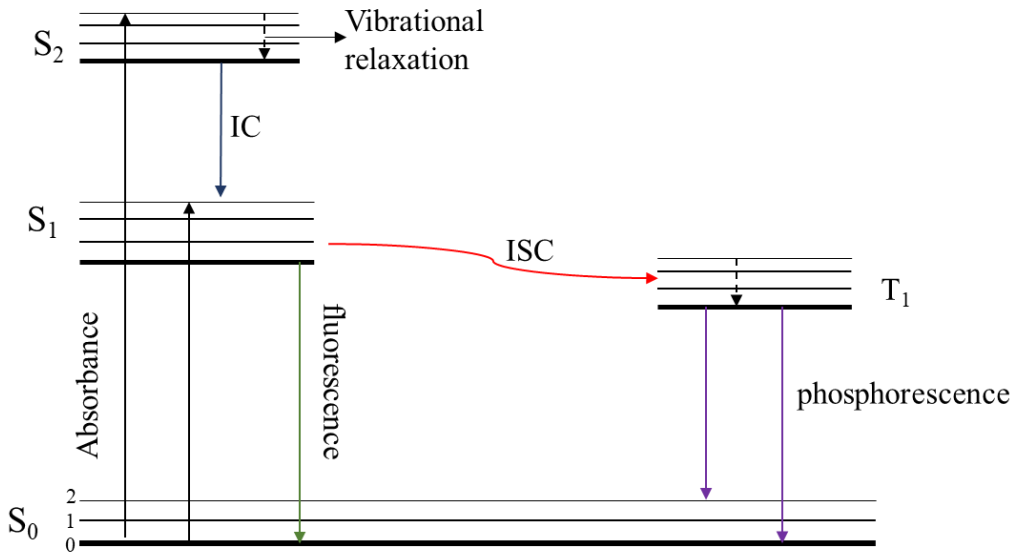

Figure 5: Jablonski diagram showing the possible occurrences in a metal complex. S_0 represents the singlet ground state. S_1 and S_2 represent the first and second singlet excited states, respectively. Within the singlet ground state S_0, there are vibrational energy states labeled 0, 1 and 2. T_1 denotes the energy level of the triplet excited state

When a molecule is placed in a light source, it absorbs a certain part of the light spectrum called the absorption spectrum of the molecule. Upon absorption of a photon, electrons within the molecule are promoted from the ground state to the highest electronically excited state. For some transition metal complexes, the ground state is usually a singlet ground state S_0 as

illustrated in figure 5.[15] Electrons move from the singlet ground state to the singlet excited states, which is the only excitation allowed according to the spin selection rule.[12] Transitions usually observed in organic molecules, metal complexes, and molecules with conjugated π systems are $\pi \rightarrow \pi^*$ and $n \rightarrow \pi^*$. Dipyrrin complexes of zinc feature absorption bands in the visible region between 400 nm and 550 nm and possess long-lived excited states which allow for electron and energy transfer processes.[16] In an electronic state, there are several vibrational states that can accommodate electrons. At an excited electronic state, the electron has the tendency to relax to the lowest vibrational energy level termed as vibrational relaxation (figure 5).

There are two types of decay process that can occur after absorption—radiative and non-radiative. Radiative decay of molecules comes in two distinct forms—fluorescence and phosphorescence. Fluorescence is the radiative decay of a molecule from the excited state to the ground state of the same spin multiplicity. This is when the singlet excited state electron returns to the singlet ground state with the emission of a photon. Fluorescence can be detected by the fluorometer or spectrofluorometer under normal conditions. For some transition metal complexes, radiationless decay from the singlet excited state to the triplet state is observed. This phenomenon is called intersystem crossing where electrons move from one state of spin multiplicity to another. It is enhanced by strong spin-orbit coupling resulting in the mixing of the excited states which relaxes the selection rules. Emission from the triplet excited state to the singlet ground state, once forbidden, therefore becomes possible.[17,18] Hence, phosphorescence is slow and is always observed at wavelengths lower than the fluorescence wavelength. For organic dyes, observation of phosphorescence intensity in an emission spectrum is very minimal under normal conditions due to factors that compete with the slow relaxation process. Among such are energy transfer, electron transfer, and non-radiative decay pathways. Measurements of

phosphorescence are therefore taken under low temperatures (77 K) using liquid nitrogen. This reduces collisions and vibrational deactivations increasing the phosphorescence intensity.[18]

Triplet State Formation

Population of the spin-forbidden localized triplet excited state from the singlet excited state is a phenomenon that is only possible for certain metal complexes. Following light absorption and promotion to the S_1 energy level, charge transfer between chromophores results in polarized excited states. Filatov gives a vivid pictorial account of the molecular orbital diagram for the photo-induced electron transfer (PET) process between electron donor and electron acceptor systems.[19] Generally, there are a number of intersystem crossing (ISC) pathways that have been studied and reported to enhance the formation of triplet state. Among them are two commonly known: the radical-pair intersystem crossing (RP-ISC) and spin-orbit charge transfer intersystem crossing (SOCT-ISC) as illustrated in figure 6.[20–22] With the RP-ISC, there is a formation of a triplet charge-transfer state intermediate from a singlet charge-transfer state. Electrons move from the triplet charge-transfer state intermediate to the localized triplet excited state. An example of a reaction process that utilizes this pathway is photosynthesis.[20] The SOCT-ISC pathway sees a direct transfer of electrons from the singlet excited state charge transfer state to the localized triplet excited state. This mechanism is especially observed in metal-organic frameworks with two or more identical and symmetric chromophores and is reported to be similar to aromatic carbonyls with $n \rightarrow \pi^*$ and $\pi \rightarrow \pi^*$ type of ISC. The major difference between the pathways lies in the proximity of the donor-acceptor species. In RP-ISC, there is weak interaction between electrons of the chromophore pair because, they are farther

apart. The chromophore pairs that are closely linked tend to go through the SOCT-ISC to form a triplet state.[20,23]

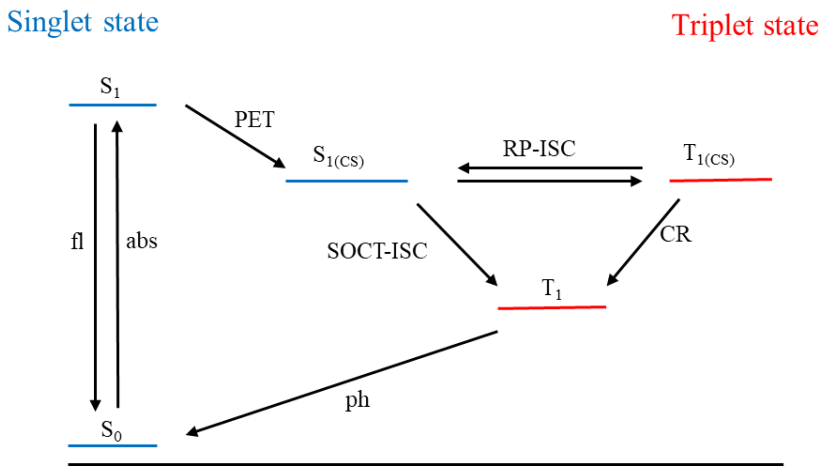

Figure 6: Diagram illustrating mechanisms of triplet state formation[22]

Fluorescence(fl), absorption (abs), phosphorescence (ph), charge recombination (CR), singlet ground state (S_0), singlet excited state (S_1), triplet excited state (T_1), singlet charge-separated state ($S_{1(CS)}$), triplet charge-separated state ($T_{1(CS)}$), photo-induced electron transfer (PET), radical-pair intersystem crossing (RP-ISC), spin-orbit charge transfer intersystem crossing (SOCT-ISC).

Complexes, especially metal complex systems, that undergo ISC may follow either of the mechanisms mentioned above and other pathways that were not cited here. Of interest to us is the SOCT-ISC which has been the mechanistic pathway reported to be employed by some metal dipyrrin complexes that are closely spaced, including zinc dipyrrin complexes in the formation localized triplet excited state.[19] The symmetric chromophores of the transition metal complexes such as homoleptic zinc dipyrrins form electron donor-electron acceptor system. Structural

geometry of complexes is of great importance here. The structure of homoleptic zinc dipyrrin complex is such that the two dipyrrin ligands on both sides are almost perpendicular (orthogonal) to each other. Trinh and co-workers measured the dihedral angles of distortion between the two dipyrrin ligands for a series of zinc dipyrrin complexes.[16] Their report shows that the dihedral angles between mean planes of the two dipyrrin ligands ranged from 76.7^{o} to 88.3^{o}.[16] The orthogonal geometry of the metal-ligand complexes compensates for the electron spin magnetic moment and orbital angular momentum interaction in the SOCT-ISC process. As electrons orbit, their motion generates a magnetic field which interacts with the electron spin magnetic moments. For symmetric orthogonal organometallics, charge recombination from the CS state changes the molecular orbital angular momentum which generates a magnetic force for the electron spin to flip forming a triplet excited state.

The efficiency of triplet state formation depends on the relaxation pathway from singlet excited state.[12] There are a number of relaxation pathways from the singlet excited state that compete. Among such are radiative decay from the singlet excited state straight to the singlet ground state and quenching of the singlet excited state by the formation of intramolecular charge-separated state, which aids in the population of the localized triplet excited state. In non-polar solvents, there is no stabilization of charges in the S_1 state. Therefore, radiative decay to the singlet ground state is observed. However, in polar environments, the singlet excited state in transition metal-organic dyads is quenched by the formation of a charge-separated state. This pathway, lower in energy than the S_1 state, reduces the CT-T_1 energy gap maximizing triplet state formation through intersystem crossing.

Dipyrrin Complexes of Zinc

Dipyrrins (dipyrromethenes) are a type of oligopyrroles specifically grouped as hemi-porphyrins.[18] They are organic molecules that possess a high number of degrees of unsaturation. This allows for delocalization of the electron density across their structure due to the presence of the conjugated π system. Photophysical properties, including stability, of dipyrrins are a function of the type and number of substituents attached to the mother structure. Hydrogens on all parts of the parent dipyrrin structure can undergo numerous forms of substitutions to finetune characteristics and properties of the molecule for specific applications. Free-base dipyrrins are bidentate ligands. The pyrrolic nitrogens seen in figure 7 serve as sites for coordination to metals, especially transition metals which have been widely exploited for various purposes and uses.[15] Dipyrrins play very key roles in biological systems such as photosynthesis, metabolism, oxygen transport, and a host of biotic redox activities.[19] A typical function is in the aspect of metabolism; dipyrrins act as metabolites of porphyrins and are part of a group of oligopyrroles called bile pigments. In photosynthesis, they serve as light absorbers due to their conjugated π system.

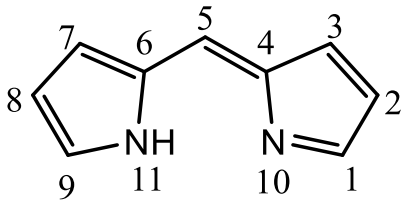

Figure 7: IUPAC-recommended numbering scheme for dipyrrin nomenclature.[24]

Positions 1 and 9 are termed as the α positions while the 5-position is known as the meso position

Metal complexes of dipyrrin ligands have attracted a lot of attention due to the diversity of applications they present. The flexibility and tunability of their structure modification allow for suitable and specific uses. Boron dipyrrin complexes, BODIPYs, have been used extensively in the areas where photochemistry plays a major role such as optical sensors, laser dyes, biomarkers, drug delivery systems, photodynamic therapy, etc.[22,25,26] They are thermally stable, have intense absorption and emission bands and high fluorescence quantum yields.[27,28] Fluorescence quantum yields reported from literature are usually very high (between 75 % and 90 %).[28–32] The major limitation to boron dipyrromethenes (BODIPYs) is the inability to form an intramolecular charge transfer leading to an ISC due to the presence of only one dipyrrin ligand attached to BF_2. Another drawback for BODIPYs is that compared to zinc dipyrrins, BODIPYs are rigid. The flexibility of zinc dipyrrins gives them an advantage in terms of structural modification and tunability.

Homoleptic zinc complexes of dipyrrin have two dipyrrin ligands in almost orthogonal position to each other with the zinc metal at the center. Intramolecular transfer of electrons can occur between the two dipyrrin chromophores forming charge separation with high oxidation-reduction potentials. Relative to the BODIPYs, dipyrromethene chelates of d-block metals have an advantage in terms of easier self-assembling at room temperature favoring them in practical applications.[33] Sazanovich *et al.*, for instance, in 2004 achieved high fluorescence in a bis(dipyrrinato)-zinc complex by replacing phenyl substituted rings at the 5,5' positions with mesityl groups (figure 8). There was a transformation in the photophysical property of the zinc complex from a weak emitter complex with a very short half-life of relaxation to a highly fluorescent chromophore with an extended singlet excited-state lifetime.[34] This substituent

replacement induced some rigidification into the zinc dipyrrin structure and eliminated non-radiative emission by the rotation of the phenyl ring.

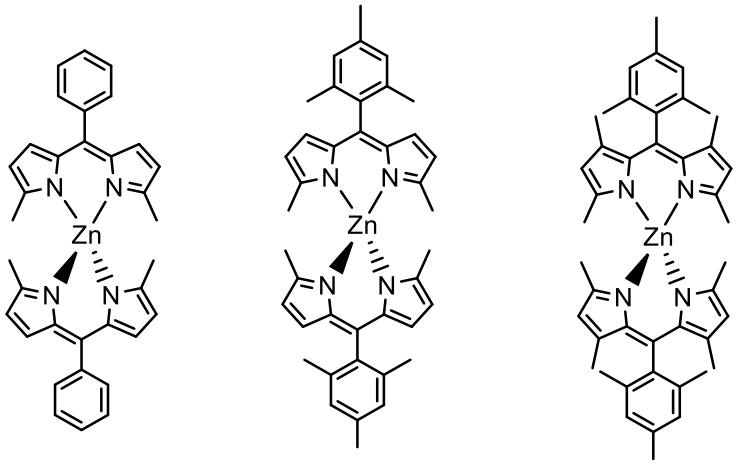

Figure 8: Zinc dipyrrins with a variety of substituents that have been studied in previous works[1,34–38]

In the zinc dipyrrin metal complex, the metal-ligand bonds are slightly polar.[16] The molecular orbitals are not equally delocalized between metal and ligands but predominantly located at the ligands. Once the metal complex absorbs light, the electron transfer that occurs at the highly polar excited state results in the creation of a charge-separated state.[19] The type of solvent used plays a very key role during emission in metal complex dyads. In polar solvents, very little fluorescent emission is observed in homoleptic zinc dipyrrin complexes due to the intramolecular transfer of charges between the dipyrrin chromophores. Formation of CS state can be attributed to the effective stabilization of charges on the dipyrrin ligands in the polar region as shown in figure 9.[16] In a polar medium, the charged complex in its excited state forms a dipole-dipole interaction with solvent molecules leading to effective stabilization of charges. The stabilization of charges in the polar medium brings the CS state to a lower energy level than the

singlet excited state which makes a forbidden phenomenon possible in this system. On the other hand, in nonpolar solvents, a variation is observed when the zinc complexes do not undergo charge separation.[19,39]

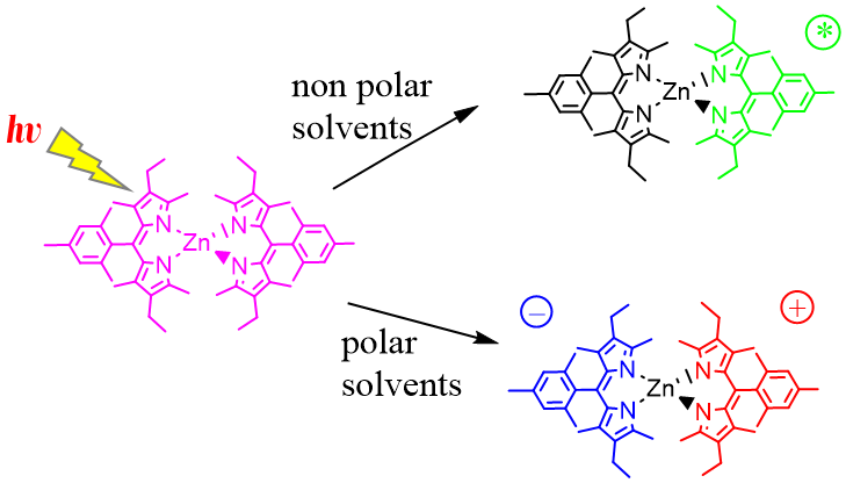

Figure 9: Pictorial illustration of the behavior of zinc complex in polar and nonpolar solvents

Previous Work

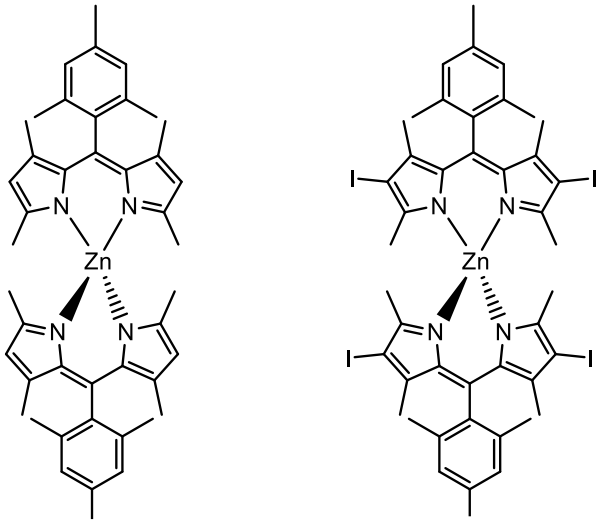

Figure 10: Previously studied zinc(II) dipyrrin photosensitizers

The above zinc dipyrrin complexes (figure 10) were synthesized and studied by Alqahtani *et al.* in quantifying the triplet state formation in photosensitizers in 2019.[39] According to Alqahtani and co-workers, though a CS state was observed in polar environments of the transition metal complexes of zinc above, the zinc complex B did not match the hypothesis, which states that the formation of a charge-separated state consequently results in a triplet state. The triplet state formation was calculated by measuring the extinction coefficient of the triplet excited state using a triplet-triplet energy transfer to perylene, an electron acceptor, against a standard sample. From the results obtained, it was established that the intramolecular $\pi \rightarrow \pi^*$ transitions were discrete rather than charge delocalization, as observed in the lowest energy triplet excited state computational calculations in both complexes.

The steady state absorption and emission energies showed very little to no change in different solvents. The fluorescence quantum yields, however, had a significant decrease moving from non-polar to polar solvents due the quenching of the S_1 state by the CS excited sate. The triplet lifetimes observed for the two zinc complexes in both non-polar toluene and polar THF solvents exceeded the minimum lifetime needed for an effective photosensitizer. The triplet excited state extinction coefficient was observed to be lower in complex A than in complex B and was independent of the solvent environment in both complexes. In the quantification of the triplet state formation, complex A almost doubled in the triplet quantum yield calculation from toluene to THF which confirms the hypothesis of fluorescence quenching through the non-radiative CS excited state pathway for transition metal-organic complexes. Complex B, on the other hand, did not agree with the hypothesis. Triplet quantum yield results were independent of solvent polarity and did not see much of an increase in value. Though the presence of a heavy atom, iodine, increased the CS state formation, there was not a positive correlation to the

formation of triplet excited state. The increase in the CS state seen did not result in the formation of triplet state signifying that triplet state formation may not go through the CS state route for this complex.

Research Aims

The overall aim of this research is to investigate the photophysical properties of bis(2,8-diethyl-1,3,7,9-tetramethyl-5-mesityl dipyrrinato) zinc (II) complex as a photosensitizer and the role of charge-separated state in the formation of long-lived triplet excited state for reductive solar catalysis. 2,8-diethyl-1,3,7,9-tetramethyl-5-mesityl dipyrrinato boron difluoride complex is used as a control for the experiment because it contains only one dipyrrin ligand and therefore cannot form a charge-separated state.

The specific objectives are to:

a. Synthesize 2,8-diethyl-1,3,7,9-tetramethyl-5-mesityl dipyrrin complexes of boron and zinc.
b. Characterize complexes using analytical techniques like NMR, mass spectroscopy, and elemental analysis.
c. Measure and compare the initial photophysical properties of BODIPY and $Zn(DIPY)_2$ complexes such as fluorescence quantum yield in solvents of variable polarities and low temperature emission.
d. Measure the transient absorption of the complexes and quantify the triplet yield.

CHAPTER 2: EXPERIMENTAL

Materials

All chemicals and reagents used were purchased from Fisher Chemical, USA. Column, FS5 spectrofluorometer, rotary evaporator, rotary vane vacuum pump, VWR-6300PC UV-Visible Double Beam Spectrophotometer were available at the Department of Chemistry, East Tennessee State University. Nuclear Magnetic Resonance (NMR), Mass Spectroscopy (HR ESI-MS), and Elemental Analysis (EA) were analytical techniques used in the characterization of the synthesized complexes. JOEL AS400 FT NMR instrument was used to analyze the complex. High-Resolution Electrospray Ionization Mass Spectrometer (HR ESI-MS) analysis was performed at Michigan State University Mass Spectrometry & Metabolomics Core where the respective samples were ionized and vaporized, and their mass-to-charge ratio measured. The percent composition of carbon, hydrogen and nitrogen from each complex were determined for the elemental analysis at Atlantic Microlab, Inc., Georgia. Boron dipyrrin and zinc dipyrrin complexes were synthesized using procedures described by Tao *et al.* and Thompson *et al.* respectively with slight modifications.[16,40]

Methodology

Synthesis of Dipyrromethane

3-Ethyl-2-4 dimethylpyrrole (1.56 mL, 15.13 mmol) and mesitaldehyde (1.14 mL, 7.75 mmol) were dissolved in 50 mL of dichloromethane. 3 drops of trifluoroacetic acid (TFA) were added to the reaction mixture while stirring under nitrogen for 6 hours. The reaction was quenched by adding 3 mL of triethylamine (TEA) to the mixture. Washing was done with a solution of saturated Na_2CO_3 (25 mL, 3 times), 0.1 M of HCl (1 time) and brine (25 mL, 1 time).

The resulting reaction mixture was dried over anhydrous Na_2SO_4, and solvent was removed by a rotary evaporator at 700 mbar, 40^oC. The product obtained was a dark yellow solid and was used for the next step without purification. NMR spectrum of the product 2,8-diethyl-1, 3, 7, 9-tetramethyl-5-mesityldipyrromethane matched that of the reported literature.[16] ^1H NMR (399.78 MHz, $CDCl_3$): δ ppm 6.82 (s, 2.00H), 5.72 (s, 0.95H), 2.36 – 2.34 (q, 5.31H), 2.26 (s, 3.51H), 2.07 (s, 6.00H), 1.99 (s, 6.73H), 1.69 (s, 5.70H), 1.05-1.01 (t, 6.39H).

Synthesis of Dipyrromethene Ligand (Dipyrrin)

Tetrahydrofuran (THF) was freshly distilled for this process. About 300 mL of THF was poured into a round bottom flask. Pieces of sodium sticks were added to the solvent in the presence of benzophenone indicator. The mixture was distilled until yellow color turned blue indicating the absence of water. The freshly distilled THF was collected into a beaker through the distillation outlet and used in the next step. Dipyrromethane ligand from the previous synthesis was dissolved in about 150 mL of distilled THF. Approximately 3.95 g of 2,3-dichloro-5,6-dicyano 1,4-benzoquinone (DDQ) dissolved in 30 mL of THF was added slowly to the dipyrromethane solution stirring under nitrogen for two hours. The reaction was quenched with 2.5 mL of triethylamine and solvent was then removed under reduced pressure. Resultant product was dissolved in 125 mL of dichloromethane and washed three times with saturated $NaHCO_3$ solution and one time with brine. The solution was dried over anhydrous Na_2SO_4 filtered. A small amount of the product was dissolved in chloroform-D and analyzed under the NMR for similarities with literature values. It was used for the next step without purification. ^1H NMR (399.78 MHz, $CDCl_3$): δ ppm 12.09 (s, 0.55H), 6.92 (s, 1.99H), 2.69 (s, 5.98H), 2.32 (s, 3.51H), 2.31 – 2.29 (q, 5.51H), 1.95 (s, 7.07H), 1.23 (s, 6.53H), 0.97-0.93 (t, 6.68H).

Synthesis of Boron Dipyrrin Complex

The boron was added on to the dipyrrin ligand by mixing boron trifluoroetherate with dipyrrin in dichloromethane in a 1:1 ratio in the basic medium and stirred overnight. After washing the complex with water and dried over anhydrous sodium sulfate, it was dried *in vacuo.* BODIPY was further purified using column chromatography with silica gel suspended in dichloromethane as the stationary phase. A percentage yield of 26% was obtained. ^{1}H NMR (399.782 MHz, $CDCl_3$): δ ppm 6.93 (s, 1.99H), 2.52 (s, 6.07H), 2.33 (s, 2.45H), 2.30 – 2.29 (q, 3.79H), 2.08 (s, 6.13H), 1.28 (s, 6.83H), 0.99-0.96 (t, 6.28H). ^{13}C NMR (100.53 MHz, $CDCl_3$): δ ppm 154.82, 142.15, 137.32, 137.20, 137.16, 136.10, 134.26, 130.76, 128.68, 21.29, 19.68, 17.16, 14.80, 12.60, 10.60. EA Calculated for $C_{26}H_{33}N_2BF_2$.0.4 CH_3OH: C, 72.86%; H, 8.01%; N, 6.44% found C,72.90%; H, 8.09%; N,6.29%. HR ESI-MS Calculated for $C_{26}H_{33}N_2BF_2$ 423.2782 $[M+H]^+$, Found: 422.2811 $[M+H]^+$.

Synthesis of Zinc Dipyrrin Complex

A solution of zinc acetate dihydrate $Zn(OAc)_2•2H_2O$ (5.13 g, 23.371 mmol) in 25 mL of methanol was prepared and added to dipyrrin ligand in methanol in the presence of TEA. The reaction mixture was stirred under air overnight. The resultant solution was filtered with a frit and the solvent removed under reduced pressure. The solid obtained was further dissolved in a minimum amount of dichloromethane and recrystallized by the addition of methanol to yield a dark-green substance. Afterwards, the solid was purified with a column filled with neutral alumina suspended in dichloromethane as the stationary phase. The resultant zinc dipyrrin complex ranged from dark-green crystals to orange powder to red powder with green crystals. Percent yield after purification was between 5 % and 13 %. ^{1}H NMR (399.782 MHz, $CDCl_3$): δ

ppm 6.91 (s, 4.32H), 2.346 (s, 6.91H), 2.250 – 2.231 (q, 9.89H), 2.100 (s, 14.27H), 1.961 (s, 14.04H), 1.178 (s, 14.98H), 0.914-0.877 (t, 15.27H). ^{13}C NMR (100.53 MHz, $CDCl_3$): δ ppm 154.82, 142.15, 137.32, 137.20, 137.16, 136.10, 134.26, 130.76, 128.68, 21.37, 19.60, 18.04, 15.40, 14.49, 11.88. EA calculated for $C_{52}H_{66}N_4Zn.2\ H_2O.\ 0.8\ CH_3OH.\ 0.2\ CH_2Cl_2$: C, 71.43%; H, 8.32%; N, 6.29% found C, 71.51%; H, 8.15%; N, 6.11%. HR ESI-MS Calculated for $C_{52}H_{66}N_4Zn$ 811.4626 $[M+H]^+$, Found: 811.4626 $[M+H]^+$.

Steady State Spectroscopy

Dilute solutions (Abs < 2) of the complexes were prepared in six different solvents and UV-Visible spectra were recorded on a VWR-6300PC UV-Visible Double Beam Spectrophotometer. Solvents included hexanes, toluene, THF, ethyl acetate, chloroform, and DCM. The double beam spectrophotometer was equipped with D_2 and W lamps controlled by the UV-VIS ANALYST software version 5.44. Wavelength scan range was set from 250 nm to 750 nm. For every new set of measurement, system baseline was calibrated, as well as the automatic blank calibration. The step of the absorbance spectra was 0.5 nm with a slit bandwidth of 2.0 nm. A one-centimeter quartz cuvette was used to help maintain the light pathlength at 1.0 cm. Absorbance measurements were taken at least three times on independently prepared samples.

Steady-state emission spectroscopic measurements of aerated complex solutions were taken on an FS5 spectrofluorometer from Edinburgh Instruments, UK using the SC-05 standard cuvette holder. The instrument is equipped with Xenon lamp as the excitation source, a PMT (R928P, Hamamatsu) detector and controlled by the Fluoracle software version 1.9.4. Excitation and emission bandwidths were both 1.0 nm. Emission scans ranged between 480 nm and 800

nm, were repeated at least three times on independently prepared samples and each emission scan was corrected for detector response.

Fluorescence Quantum Yield

$Zn(DIPY)_2$ and BODIPY complexes were analyzed for their fluorescence quantum yields. Dilute solutions of complexes were prepared in six solvents—n-hexane, toluene, ethyl acetate, THF, chloroform, and DCM—and absorbance was first taken using VWR-6300PC UV-Visible Double Beam Spectrophotometer to ensure the excitation wavelengths were recorded between the absorbances of 0.1 and 0.2. Emission spectra of the same complex solutions were then taken with an FS5 spectrofluorometer. Excitation absorbances were recorded at 480 nm for all solutions of the zinc dipyrrin complex, and 499 nm for that of boron dipyrrin complex. Emission scans ranged from 490 nm to 820 nm for $Zn(DIPY)_2$ and from 510 nm to 820 nm for BODIPY. Emission spectra for the sample solution, standard solution, standard solvent, and sample solvent were measured and corrected. Tris-(bipyridine) ruthenium(II) chloride $[Ru(bpy)_3]Cl_2$ in aerated water was used as the standard for the quantum yield measurements (quantum yield of the reference is 0.040)[41]. The fluorescence quantum yield was calculated using the equation below where Φ_F is fluorescence quantum yield of complex, Φ_{std} is fluorescence quantum yield of standard, I_{unk} is intensity of unknown (complex), I_{std} is intensity of standard, A is absorbance at excited wavelength and η is the refractive index[42]

$$\Phi_F = \Phi_{std}\left(\frac{A_{std}}{A_{unk}}\right)\left(\frac{I_{unk}}{I_{std}}\right)\left(\frac{\eta_{unk}}{\eta_{std}}\right)^2 \qquad (3\text{-}1)$$

Low Temperature Emission

Emission spectra of complexes were studied at 77K using liquid nitrogen. Data was collected using FS5 spectrofluorometer from Edinburgh Instruments, UK with an SC-70 Liquid Nitrogen Dewar cuvette holder. Diethyl ether, 2-methyl THF, and propionitrile-butyronitrile (4:5) were the solvents used for this analysis. They form optical glasses when frozen for efficient analysis. The sample transferred into an NMR tube was submerged in liquid nitrogen in the sample chamber to freeze the solutions of dipyrrin complexes. Long pass filters (LP 470 nm and LP 660 nm) were placed after the sample to minimize scattering. Emission scans were taken and corrected for detector response.

CHAPTER 3: RESULTS AND DISCUSSION

Synthesis and Characterization of Dipyrrin Complexes

The synthesis of bis(2, 8-diethyl-1, 3, 7, 9-tetramethyl-5-mesityldipyrrinato) zinc(II) was a straightforward procedure where mesityladehyde reacted with 3-ethyl-2-4 dimethylpyrrole in the presence of trifluoroacetic acid for 6 hours under nitrogen to produce 2, 8-diethyl-1, 3, 7, 9-tetramethyl-5-mesityldipyrromethane ligand as performed by Thompson *et al* in 2014.[16] This ligand was oxidized with DDQ in freshly distilled THF by slowly adding DDQ-THF solution to the dipyrromethane ligand for 2 hours to form 2, 8-diethyl-1, 3, 7, 9-tetramethyl-5-mesityldipyrrin ligand. The resultant product was washed with saturated $NaHCO_3$ and brine, and dried—first over anhydrous Na_2SO_4 and later with a rotary vane pump. ^1H NMR was analyzed after each stage of synthesis to ascertain the product of the synthetic process.

Bis(2, 8-diethyl-1, 3, 7, 9-tetramethyl-5-mesityldipyrrinato) zinc(II) was finally obtained by adding a solution of zinc acetate dihydrate $Zn(OAc)_2 \bullet 2H_2O$ in methanol to the dipyrrin ligand (dissolved in methanol) in the presence of excess triethylamine. This process took place overnight under air. The end product was filtered using a frit and methanol was removed from the product solution with a rotary evaporator. The complex was purified with a column filled with neutral alumina solution as the stationary phase and dichloromethane as the mobile. The product was recrystallized afterwards to obtain a dark-green zinc dipyrrin complex. After three trials, the percent yield varied from 5 % to 13 % while the colors ranged from dark-green through orange to red. In their publication, Thompson and co-workers recoded a total percentage yield of 8-13 % their dipyrrin complexes.[16] This falls in line with resultant yields obtained in the McCusker lab for the zinc dipyrrin complex. Zinc (II) dipyrrin complex is a stable complex and has a good shelf life; however, over the period, it was observed that the moisture content

increased when left on the shelf for a very long time. It was therefore dried each time before further analysis were carried out. Figure 11 gives a systematic procedure of the synthetic route of zinc(II) dipyrrin complex.

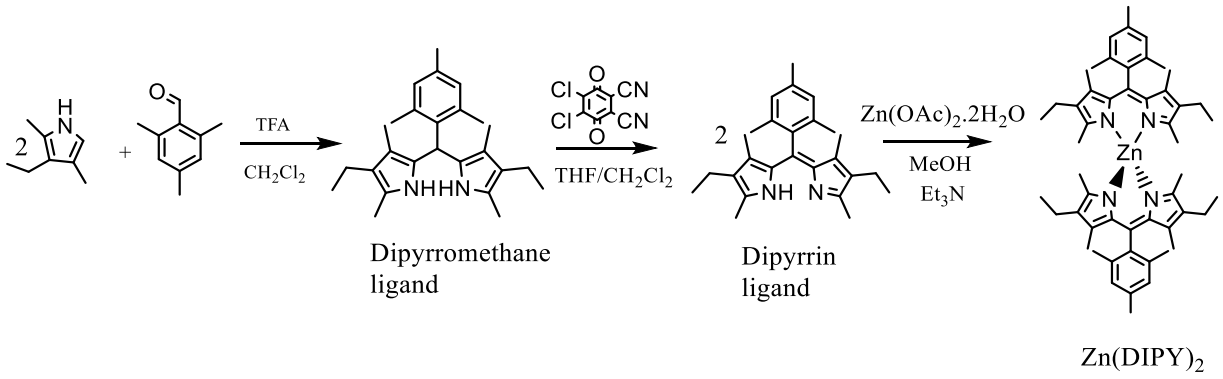

Figure 11: Synthesis of zinc dipyrrin complex

The first analytical tool employed for characterizing complexes was NMR using the JOEL AS400 FT NMR instrument. A small amount of the zinc complex was dissolved in chloroform-D and poured into an NMR tube for analysis. Detailed results of the NMR analysis for dipyrrinato zinc (II) complex are shown in figures 12 and 13. Figure 12 shows the ^{1}H NMR peaks which matched what was recorded in literature by Thompson *et al.*[16] The aromatic protons on the mesityl ring showed a peak at 6.91 ppm, the ethyl groups were located between 2.23 ppm and 2.25 ppm. The methyl groups showed singlet peaks from 0.87 ppm to 2.34 ppm. Figure 13 also shows the ^{13}C NMR peaks of the aliphatic (upfield) and aromatic carbons (further downfield).

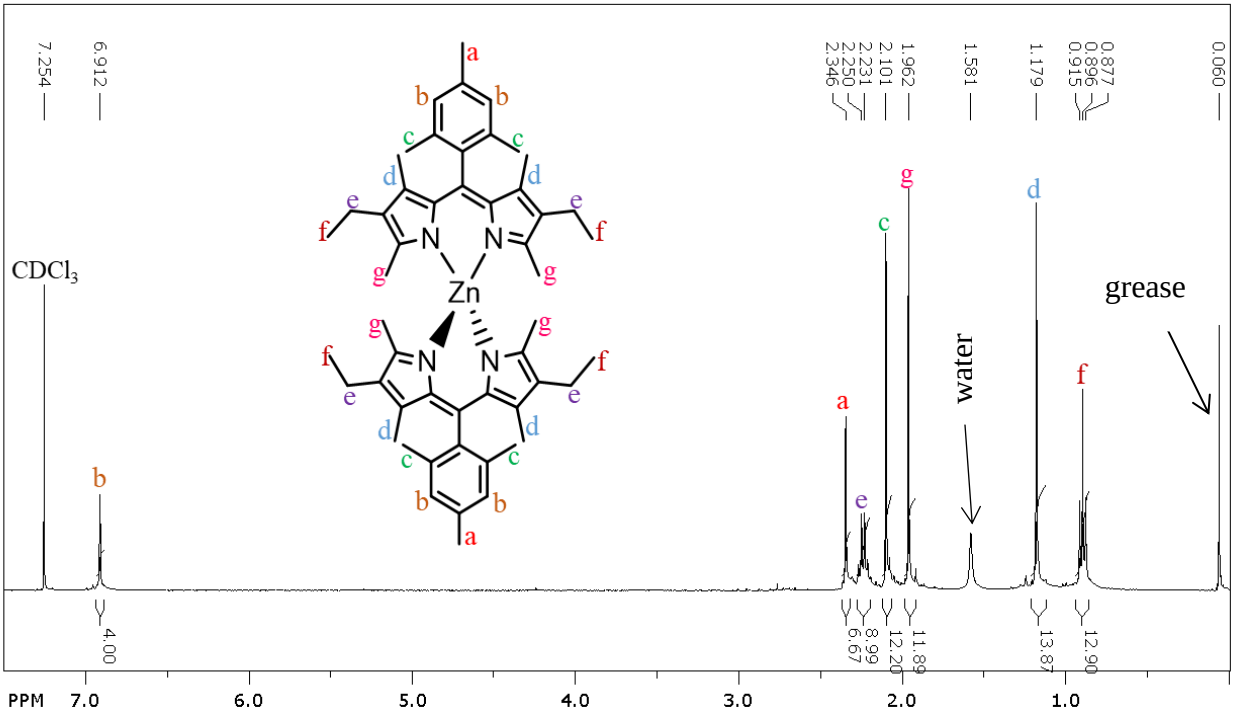

Figure 12: ^{1}H NMR of Zn(DIPY)$_2$ analyzed in CDCl$_3$

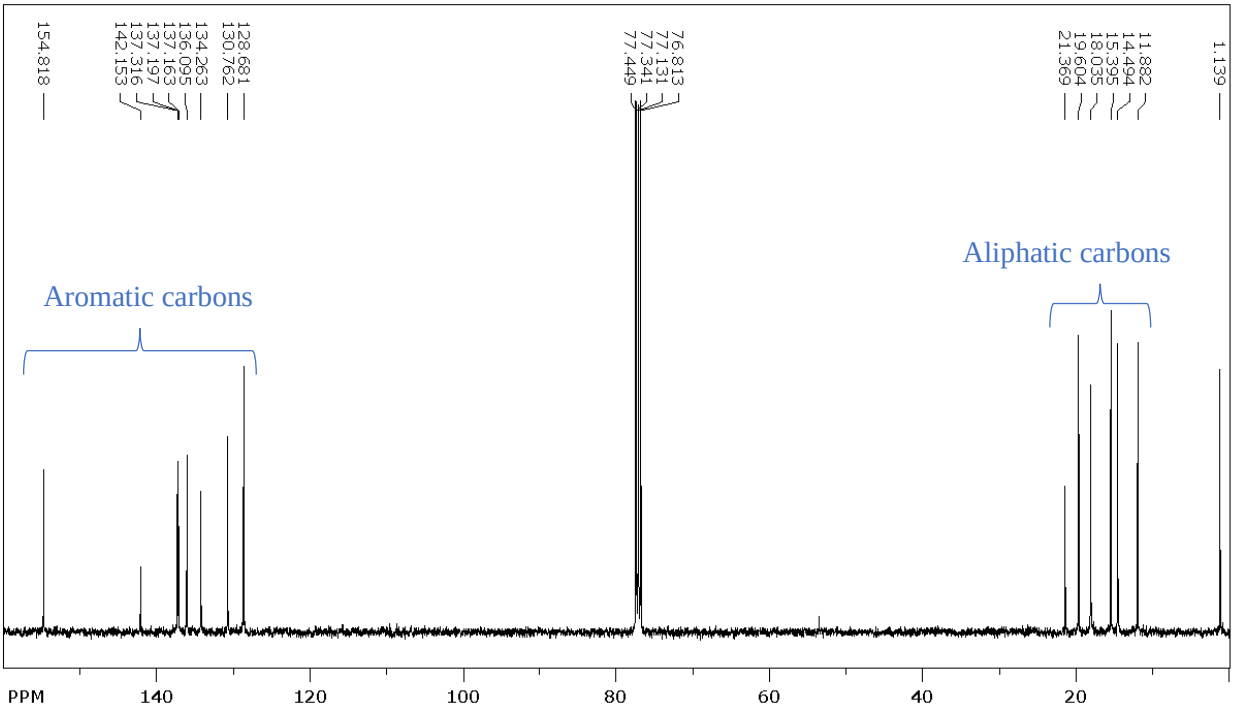

Figure 13: ^{13}C NMR of Zn(DIPY)$_2$ analyzed in CDCl$_3$

Boron Dipyrrin Complex

The initial stages of the synthesis of the ligand were done exactly as outlined in the synthesis of the zinc dipyrrin complex. Mesityladehyde was mixed with 3-ethyl-2-4 dimethylpyrrole in the presence of trifluoroacetic acid for 6 hours under nitrogen to produce 2, 8-diethyl-1, 3, 7, 9-tetramethyl-5-mesityldipyrromethane ligand.[16] The dipyrromethane ligand was oxidized with DDQ in freshly distilled THF to obtain 2, 8-diethyl-1, 3, 7, 9-tetramethyl-5-mesityldipyrrin ligand. To form the boron dipyrrin complex, boron trifluoroetherate was added to dipyrrin in dichloromethane in a 1:1 ratio in the basic medium and stirred overnight. BODIPY was further purified using column chromatography with silicon dioxide as the stationary phase and dichloromethane as mobile phase. A percentage yield of 26% was obtained. BODIPY is a very stable red powdery complex. Figure 14 shows a schematic synthetic process of boron dipyrrin complex. Figures 15 and 16 show the ^{1}H and ^{13}C NMRs results, respectively, which were in line with literature.[43]

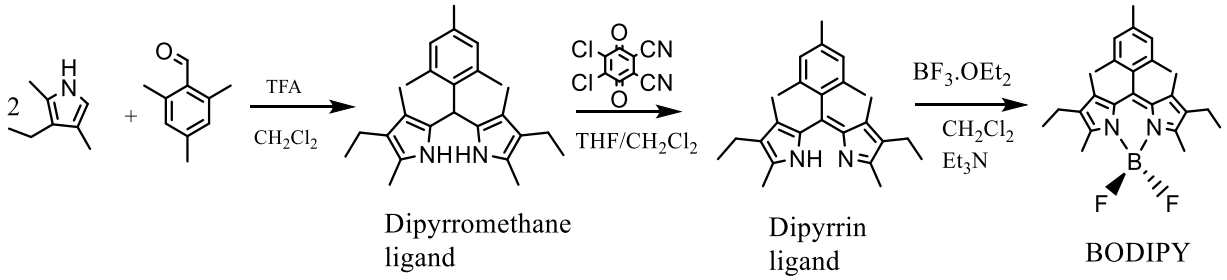

Figure 14: Synthesis of BODIPY

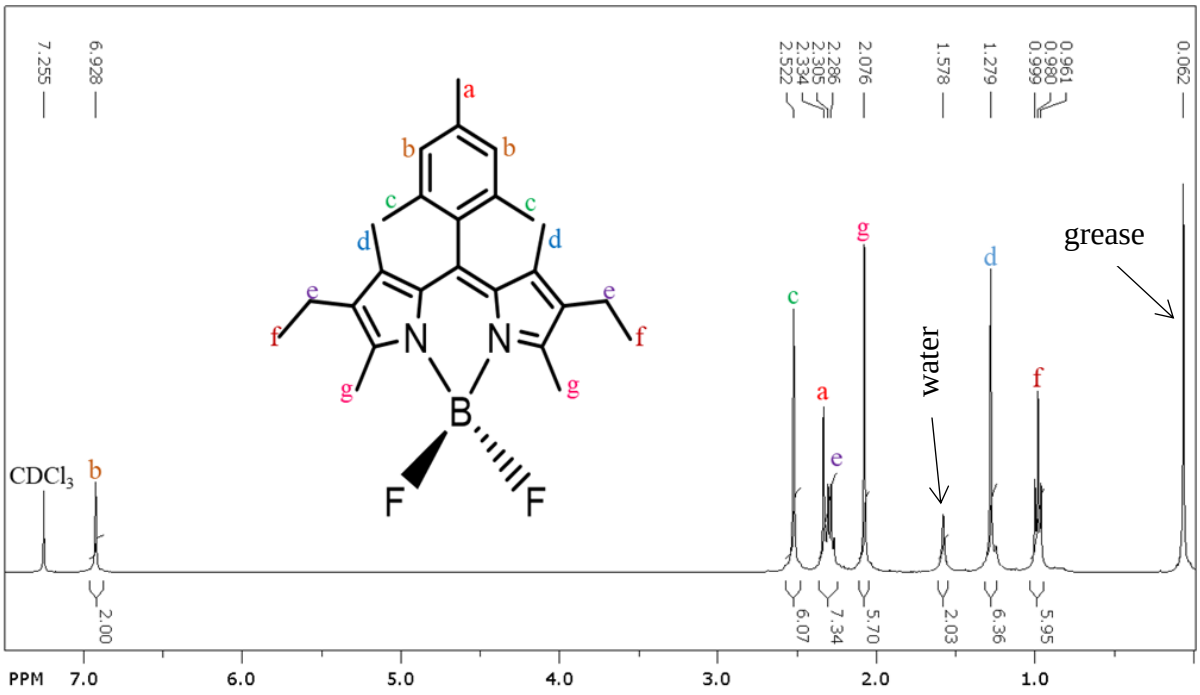

Figure 15: ^{1}H NMR of BODIPY analyzed in $CDCl_3$

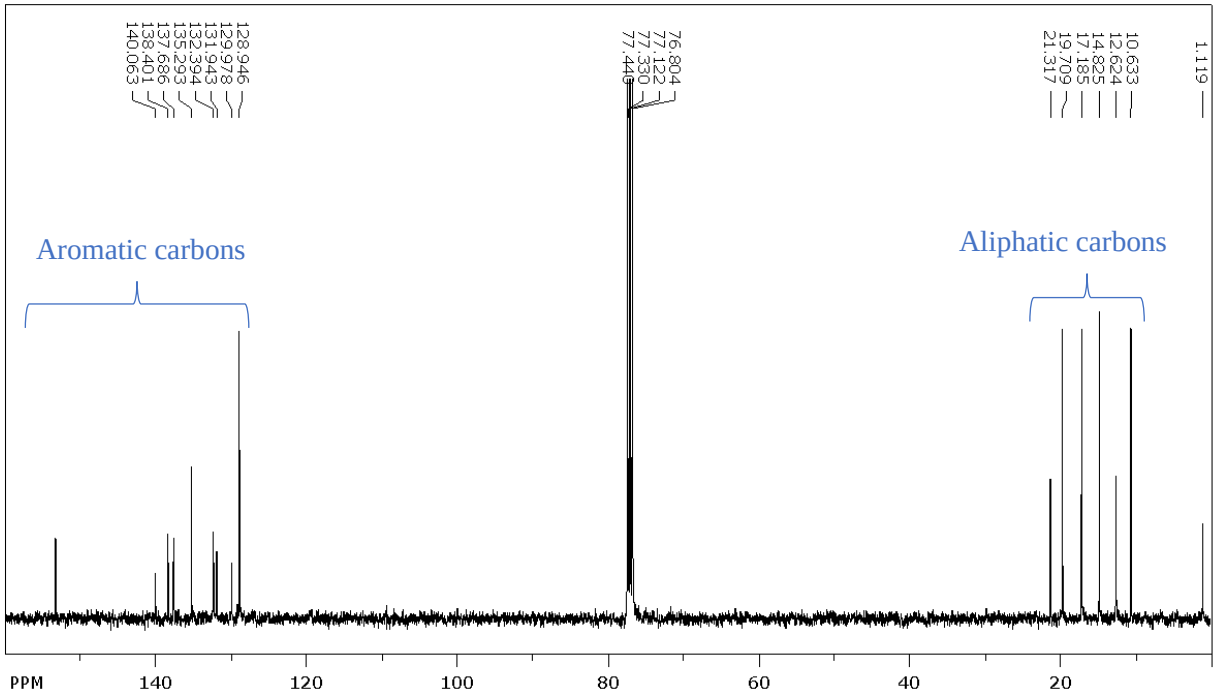

Figure 16: ^{13}C NMR of BODIPY analyzed in $CDCl_3$

Absorption Spectroscopy

Solutions of $Zn(DIPY)_2$ and BODIPY were exposed to a light source in the UV-Visible spectrophotometer equipped with D_2 and W lamps. As radiation passed through the complex solutions, they absorbed light at respective wavelengths. Electrons therefore moved from the singlet ground state S_0 to the singlet excited state S_1 in both $Zn(DIPY)_2$ and BODIPY. Absorption spectra of both complexes under study were taken in six different solvents of different polarities and their absorbance maxima of are tabulated in table 1. The solvent polarity indicator is based on the Dimroth-Reichardt E_T30 polarity scale. The E_T30 polarity scale is defined as a measure of the electronic transition energy of the pyridinium N-phenolate betaine dye in a particular solvent.[44] It is measured in kilocalories per mole at 25^0C and 1bar. A high E_T30 value corresponds to a high solvent polarity and vice versa.[45]

Table 1: Absorption and Emission Maxima of Complexes in Different Solvents

Solvent	E_T30(kcal/mol)	λ_{abs} (max/nm)		λ_{em} (max/nm)	
		$Zn(DIPY)_2$	BODIPY	$Zn(DIPY)_2$	BODIPY
n-Hexane	31.0	504.0	523.5	533.0	539.0
Toluene	33.9	507.0	527.0	534.0	543.0
THF	37.4	504.5	524.0	535.0	541.0
Ethyl acetate	38.1	503.5	522.5	533.0	540.0
Chloroform	39.1	506.0	527.0	534.0	543.0
DCM	40.7	505.5	525.0	535.0	543.0

The UV-Vis absorption maxima observed for bis(2, 8-diethyl-1, 3, 7, 9-tetramethyl-5-mesityldipyrrinato) zinc(II) $Zn(DIPY)_2$ ranged from 503.5 nm in ethyl acetate to 507.0 nm in toluene. According to Alqahtani in 2018, the absorption maximum for bis(1, 3, 7, 9-tetramethyl-5-mesityldipyrrinato) zinc(II) ZnDPY complex in toluene was recorded at 490 nm.[1] Thompson and coworkers in 2014 also reported a range of absorption maxima for bis(1, 3, 7, 9-tetramethyl-5-mesityldipyrrinato) zinc(II) in different solvents from 488 nm in DCM, 489 nm in cyclohexane and THF, to 491 nm in toluene. For the same solvents, they recorded slightly higher values of absorption maxima in bis(2, 8-diethyl-1, 3, 7, 9-tetramethyl-5-mesityldipyrrinato) zinc(II) complex—between 505 nm in THF and 508 nm in toluene.[16] The bathochromic shift of the UV-Vis spectra observed can be attributed to the presence of ethyl substituents at the 2,8 positions of the $Zn(DIPY)_2$ complex. Introduction of the electron-donating auxochromes lowered the energy gap between the HOMO and LUMO of the $Zn(DIPY)_2$ complex causing the shift in the absorbance maxima. Figure 17 shows the position of the ethyl substituents.

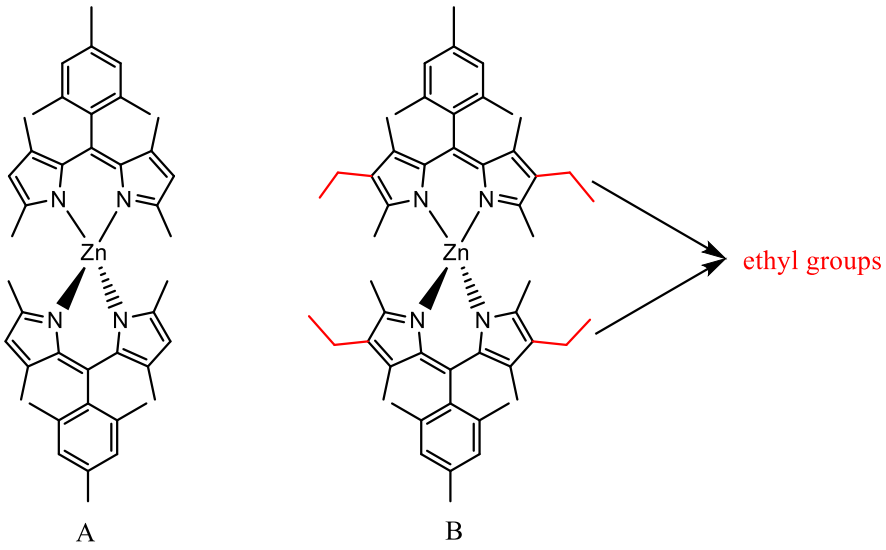

Figure 17: Diagram of zinc complexes

A similar trend was observed for BODIPY complex. Tao *et al.* in their article published in 2019 reported the UV-Vis absorption spectra of 502 nm for 1, 3, 7, 9-tetramethyl-5-mesityldipyrrinato boron difluoride in DCM.[40] Adding of the ethyl substituents onto the complex effected a red shift. The absorbance maxima recorded in the McCusker lab therefore ranged from 523.5 nm to 527.0 nm. The strong single unresolved absorption band observed in both complexes are characteristic of $\pi \rightarrow \pi^*$ transitions. These single intense peaks were assigned to the excitation of an electron from $S_0 \rightarrow S_1$.

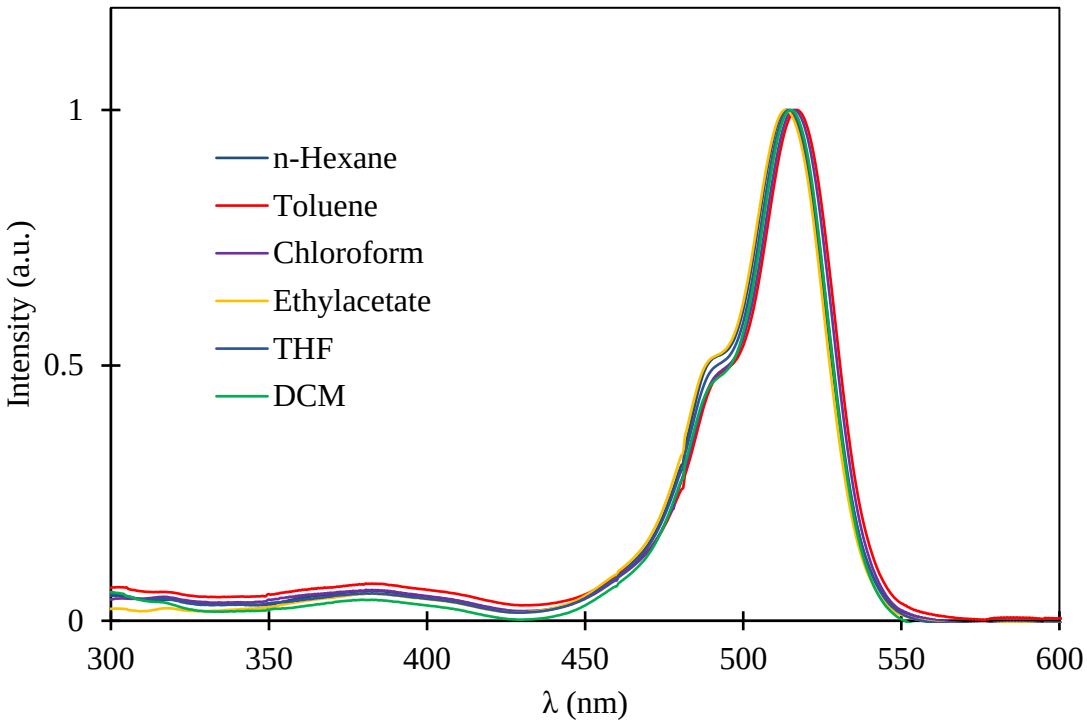

Figure 18: Normalized absorption spectra of $Zn(DIPY)_2$

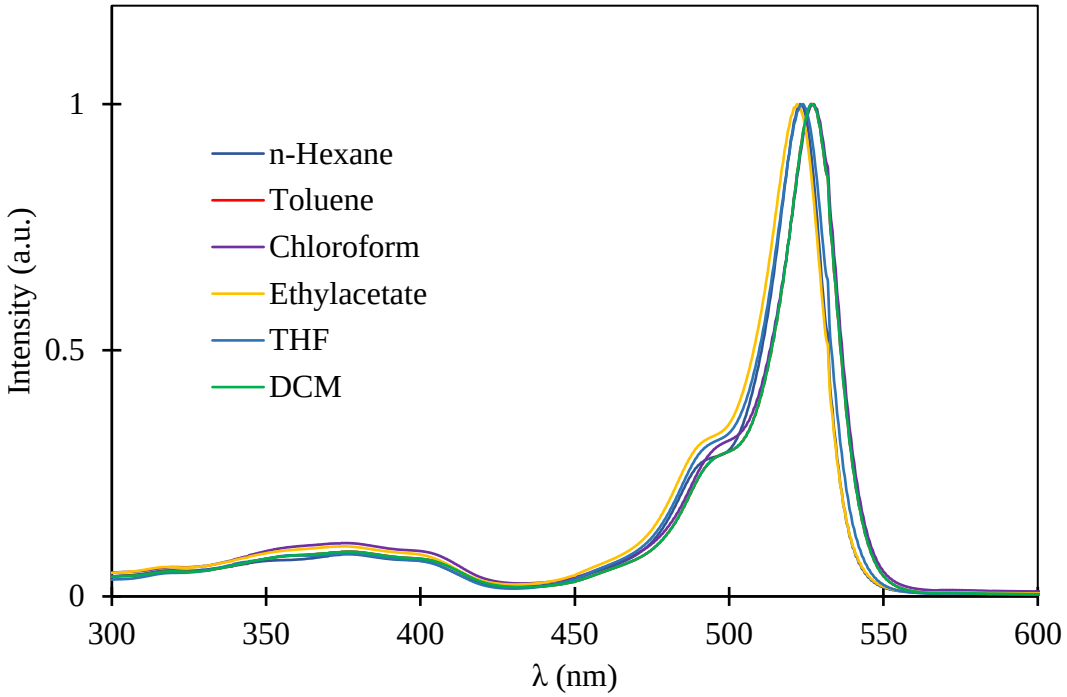

Figure 19: Normalized absorption spectra of BODIPY

Emission Spectroscopy

The steady-state emission spectroscopic measurements of $Zn(DIPY)_2$ and BODIPY were measured at room temperature in all six solvents used for previous UV-VIS analysis with emission maxima results displayed in table 1. $Zn(DIPY)_2$ was found to emit light from 533.0 nm to 535.0 nm while BODIPY emitted light from 539.0 nm to 543.0 nm. Similar to the UV-Visible spectra, the emission spectra maxima of the complexes also red shifted in the spectra results relative to their respective methyl-substituted counterparts.

Unlike the absorption spectra, there were variations in the emission spectra of $Zn(DIPY)_2$ moving from one solvent to the other. Emission spectra of the zinc dipyrrin in DCM (polar

solvent) particularly showed a shoulder between 600 nm and 800 nm as shown in figure 20. Emission at the longer wavelength can be attributed to the charge-separated state[16] experienced in polar solvents by the $Zn(DIPY)_2$ complex. Most fluorophores have larger dipole moments in the excited state than in the ground state. Therefore, at the excited state, the charge-separated state intermediate of $Zn(DIPY)_2$ interacts with the polar solvent molecules. The CS state is therefore effectively stabilized in the polar solvent lowering the energy gap between the CS state and the triplet excited state. Intersystem crossing to the triplet excited state is enhanced, followed by radiative emission from the triplet excited state to the singlet ground state. The polar solvent effect is not experienced in BODIPY, on the other hand. There was intense emission in the fluorescence region in all solvents for BODIPY as shown in figure 21.

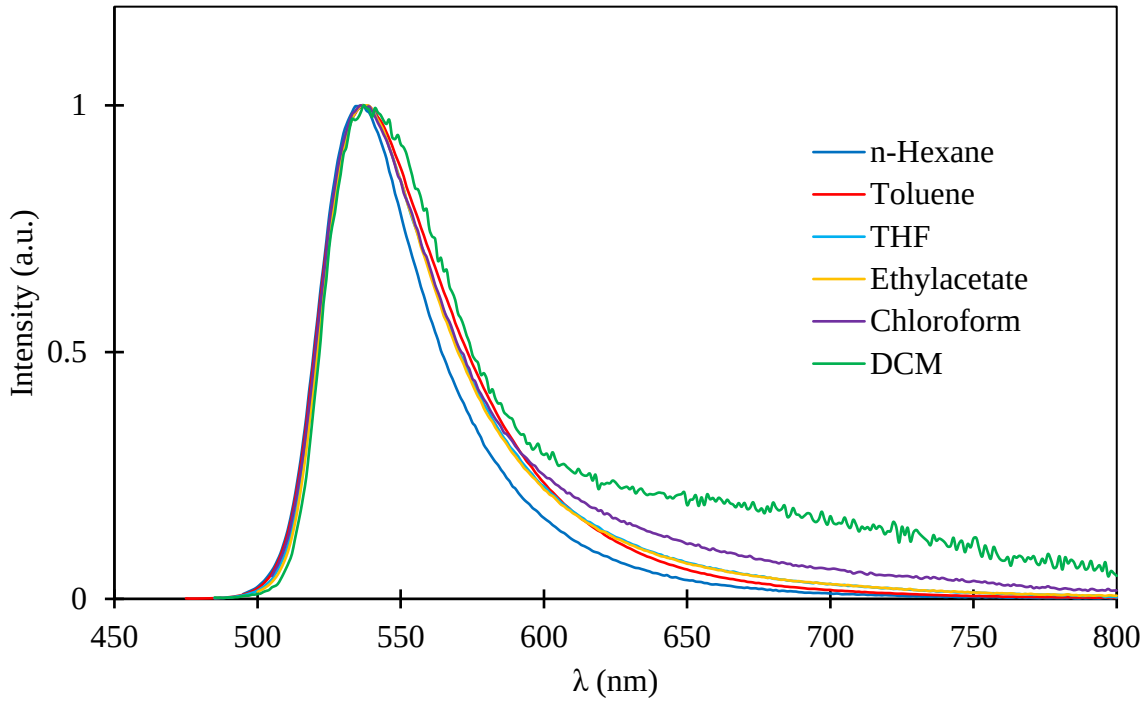

Figure 20: Normalized emission spectra of $Zn(DIPY)_2$

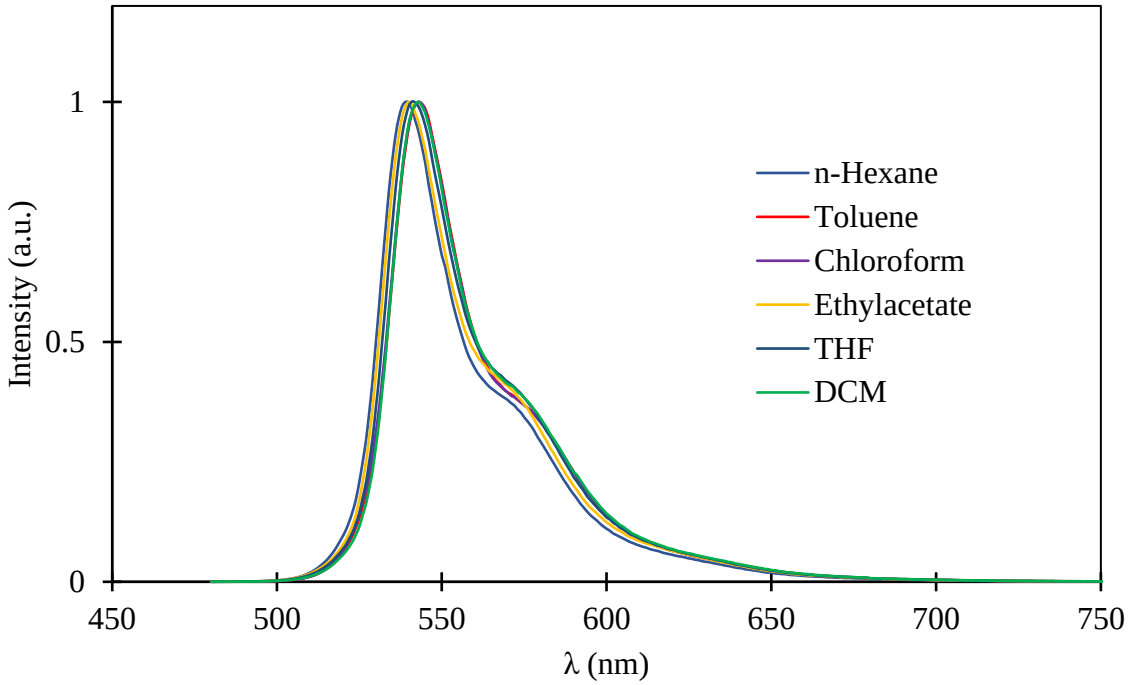

Figure 21: Emission spectra of BODIPY in various solvents

Fluorescence Quantum Yield

As mentioned earlier in chapter 1, there are generally a number of decay pathways for an excited molecule. The two fundamental pathways are radiative and non-radiative deactivation pathways. Fluorescence quantum yield measures the amount of light emitted from an excited species upon return to the ground state. The fluorescence quantum yield values of $Zn(DIPY)_2$ and BODIPY in varied solvents have been tabulated in table 2. $[Ru(bpy)_3]Cl_2$ in aerated water ($\Phi = 0.04$)[41] was used as standard. $Zn(DIPY)_2$ was excited at 480 nm for all solvents while BODIPY was excited at 499 nm for the same solvents.

Table 2: Fluorescence Quantum Yield Values of $Zn(DIPY)_2$ and BODIPY Complexes

Solvent	$Zn(DIPY)_2$	SD %	BODIPY	SD %
n-Hexane	0.212	3.471	0.854	3.037
Toluene	0.177	1.729	0.867	8.873
THF	0.033	3.535	0.858	4.849
Ethyl acetate	0.023	4.174	0.811	3.062
Chloroform	0.012	4.949	0.821	3.410
DCM	0.003	21.651	0.836	4.397

The results obtained shows that BODIPY is highly fluorescent emitting almost 90% of absorbed light, while $Zn(DIPY)_2$ emitted only about 20 % of light absorbed in n-hexane while it emitted about 0.2 % in DCM. The fluorescence quantum yield can be close to unity if the non-radiative decay rate is much smaller than the rate of radiative decay.[15] The fluorescence quantum yield for BODIPY was independent of solvent polarity; there was no stabilization of charges observed in polar solvents. For $Zn(DIPY)_2$, however, the quantum yield values recorded were a proof of heavy dependence on solvent polarity. The fluorescence quantum yield values decreased accordingly as solvent polarity increased, confirming the formation of a CS state which quenches the singlet excited state of the $Zn(DIPY)_2$ in highly polar solvents. Figure 22 gives a trend in the fluorescence quantum yield values with solvent for the respective complexes.

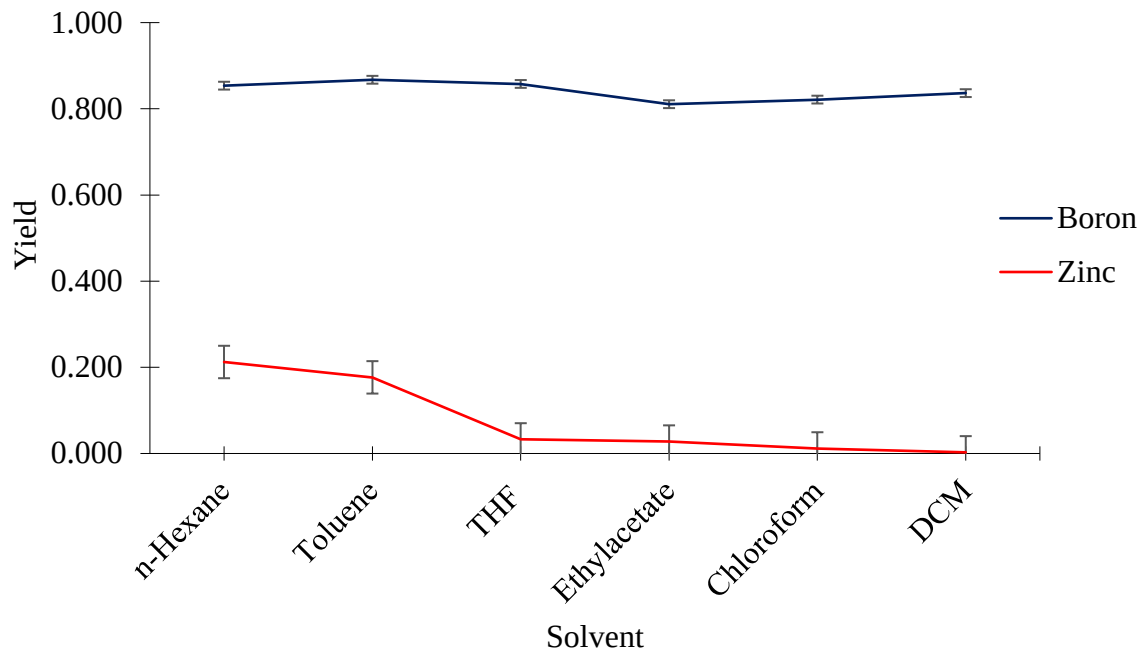

Figure 22: Plot of fluorescence quantum yield values of solvents from nonpolar to most polar

Low Temperature Emission Spectroscopy

A photoinduced electron transfer from donor D to acceptor A results in the formation of a charge-separated state which consists of the corresponding radical cation and anion, and the process is in direct competition with the radiative and nonradiative deactivation processes.[46] After the formation of a CS state, there are further decay processes that kinetically compete with emission. Due to the competition, phosphorescence is usually not seen at room temperature. Figure 23 shows a graph of emission spectra of $Zn(DIPY)_2$ observed at 77 K using liquid nitrogen. From the graph, emission was observed at longer wavelengths between 700 nm and 750 nm in the most polar solvent (propionitrile-butyronitrile). At low temperatures, molecular

vibrations and collisions are reduced increasing the phosphorescence intensity. Figure 24 shows the optimized phosphorescence signal of the emission spectra. Phosphorescence is not observed in BODIPY because there is no formation of a CS state (due to the absence of a donor-acceptor system) as seen in figure 25.

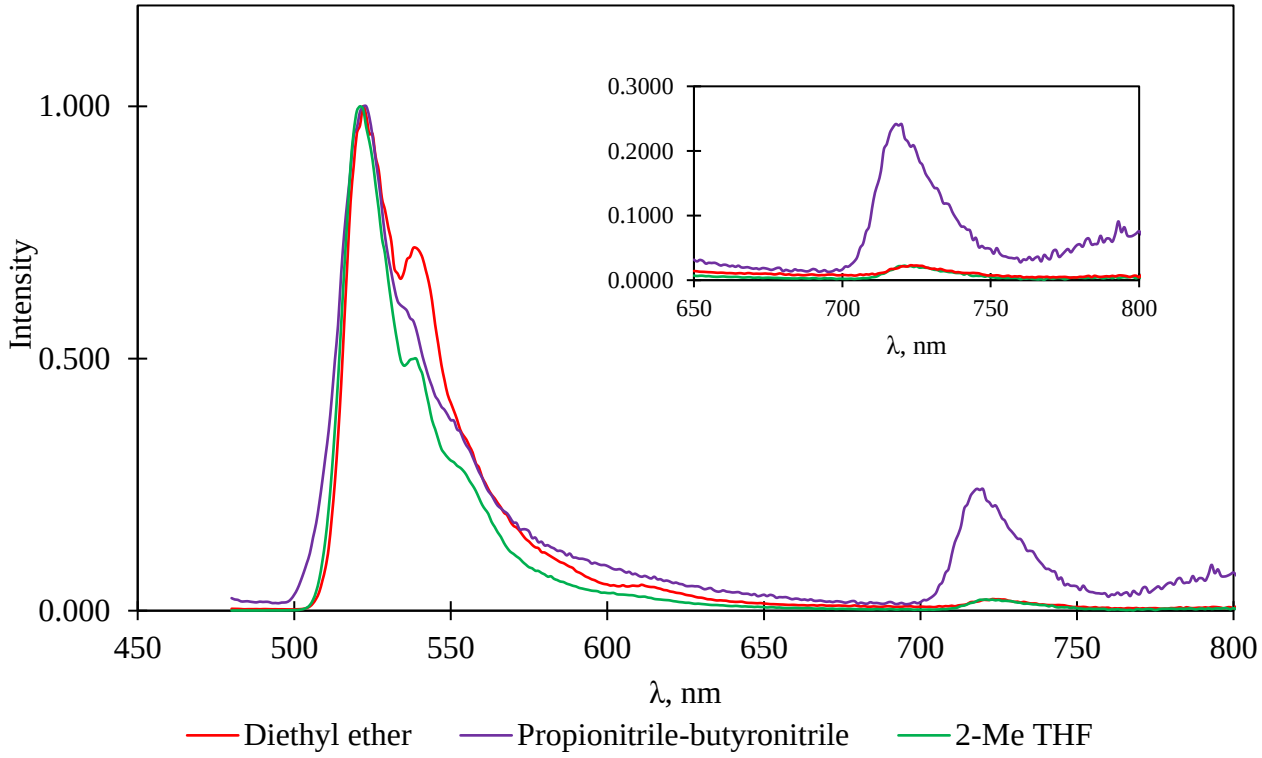

Figure 23: Normalized low temperature emission spectra for $Zn(DIPY)_2$

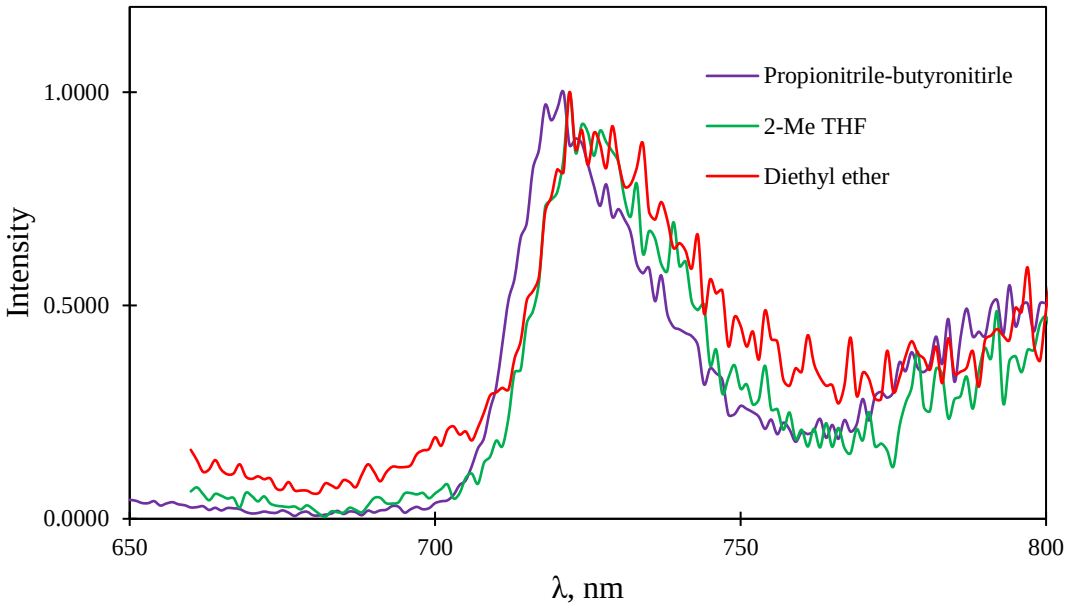

Figure 24: Normalized low temperature emission spectra of $Zn(DIPY)_2$ showing the phosphorescence region

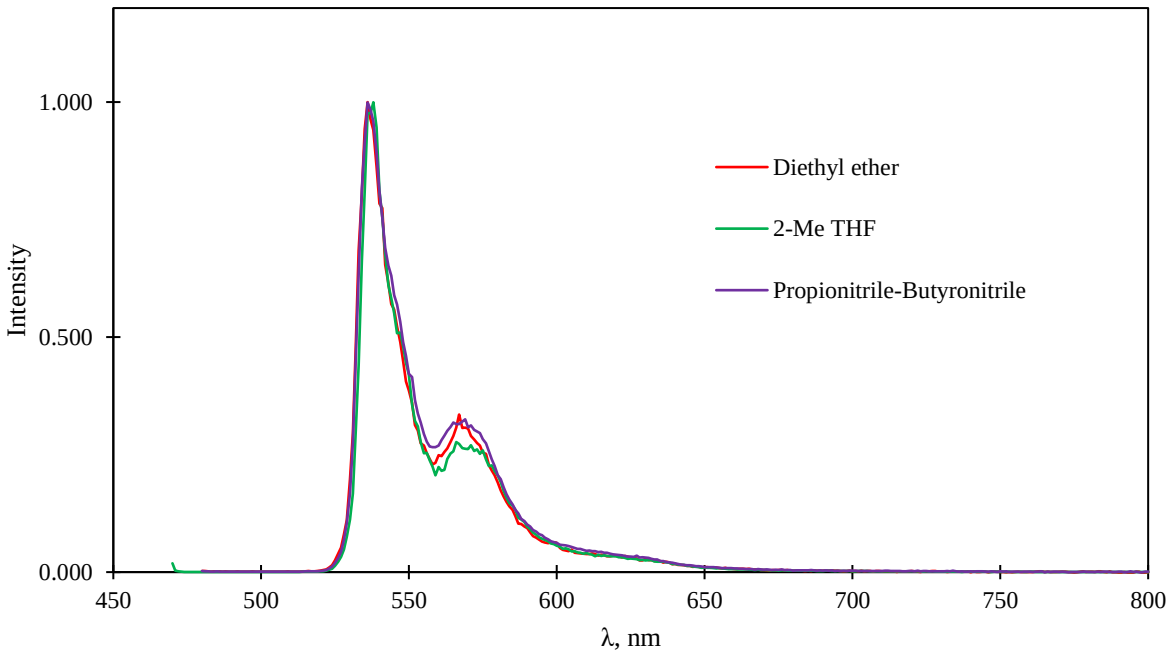

Figure 25: Low temperature emission spectra for BODIPY

CHAPTER 4: CONCLUSION

Reductive photocatalysis of CO_2 has long gained attention, with biomolecular photocatalysis requiring a photosensitizer to facilitate completion of the reaction cycle. The efficiency of a photosensitizer depends on its ability to form stable excited states with extended lifetimes long enough to allow for photochemical reactions. Extensive studies into zinc dipyrrins for a variety of applications have been done due to the ease in their syntheses and ability to finetune their photophysical properties for specific uses. Nevertheless, the use of zinc dipyrrins as efficient photosensitizers requires further research.

Previous findings from the McCusker lab performed by Norah Alqahtani showed that ZnDPY and ZnIDPY were good candidates for photosensitizers because their triplet excited state lifetimes exceeded the minimum requirement for an effective photosensitizer. However, the findings showed that ZnDPY followed the $S_1 \rightarrow CS \rightarrow T_1$ route but ZnIDPY did not obey the pattern. The presence of the iodine increased the CS formation and lowered the fluorescence quantum yield in the polar solvent. Though the triplet quantum yield also increased in the presence of the heavy atom, the yield was independent of solvent polarity. This research therefore sought to investigate the role of the CS state in the formation of triplet excited state in a more alkyl substituted zinc dipyrrin.

Bis(2,8-diethyl-1,3,7,9-tetramethyl-5-mesityl dipyrrinato) zinc (II) and 2,8-diethyl-1,3,7,9-tetramethyl-5-mesityl dipyrrinato boron difluoride complexes were synthesized, purified, dried completely, and characterized using NMR, HR ESI-MS, and EA before analyses of their photophysical properties were performed. The absorbance spectroscopy of $Zn(DIPY)_2$ ranged between 503 nm and 507 nm while that of BODIPY ranged between 522 nm and 527 nm. Steady-state emission spectroscopy for $Zn(DIPY)_2$ was from 533 nm to 535 nm whereas

emission maxima for BODIPY was from 539 nm to 543 nm. The fluorescence quantum yield for BODIPY was very high emitting about 87% of radiation, confirming the numerous studied performed on boron dipyrrin complexes as highly fluorescent. Relatively, the highest fluorescence quantum yield value recorded for $Zn(DIPY)_2$ was 21% in hexane. The value decreased accordingly as the solvent polarity increased. In DCM, a fluorescence quantum yield value of 2.7% was calculated. The results proved the stabilization of the CS state in $Zn(DIPY)_2$. Low temperature emission of $Zn(DIPY)_2$ was measured in three solvents with different polarities. Results showed that emission was observed at the phosphorescence region between 700 nm and 750 nm in the most polar solvent. This signifies that the local triplet excited state was populated, and hence radiative emission from T_1 to S_0 was observed as 77 K.

Future Research

Transient absorption analysis and the triplet quantum yields of $Zn(DIPY)_2$ and BODIPY are currently being measured by our collaborators at North Carolina State University. This will help determine the quenching route for the $Zn(DIPY)_2$. Furthermore, syntheses, characterization, and analysis of the photophysics of 1, 3, 7, 9-tetramethyl-5-mesityl dipyrrinato boron difluoride (BoMeDIPY) and 2, 8- diiodo-1, 3, 7, 9- tetramethyl-5-mesityl dipyrrinato boron difluoride (Bo-I-DIPY) will be carried out to validate the importance of the CS state in the formation of the triplet excited state.

REFERENCES

(1) Alqahtani, N. Synthesis and Characterization of Zinc(II) Dipyrrin Photosensitizers. *Electron. Theses Diss.* **2018**, 66. https://dc.etsu.edu/etd/3466.

(2) Lingampalli, S. R.; Ayyub, M. M.; Rao, C. N. R. Recent Progress in the Photocatalytic Reduction of Carbon Dioxide. *ACS Omega* **2017**, *2* (6), 2740–2748. https://doi.org/10.1021/acsomega.7b00721.

(3) Center for Sustainable Systems, University of Michigan. "U.S. Energy System Factsheet." Pub No. CSS03-11. 2019.Pdf.

(4) *Climate Change 2014: Impacts, Adaptation, and Vulnerability: Working Group II Contribution to the Fifth Assessment Report of the Intergovernmental Panel on Climate Change*; Field, C. B., Barros, V. R., Intergovernmental Panel on Climate Change, Eds.; Cambridge University Press: New York, NY, 2014.

(5) Qin, Z.; Su, T.; Ji, H.; Jiang, Y. Photocatalytic Reduction of Carbon Dioxide. In *Hydrogen Production and Remediation of Carbon and Pollutants*; Lichtfouse, E., Schwarzbauer, J., Robert, D., Eds.; Environmental Chemistry for a Sustainable World; Springer International Publishing: Cham, 2015; Vol. 6, pp 61–98. https://doi.org/10.1007/978-3-319-19375-5_2.

(6) Inventory of U.S. Greenhouse Gas Emissions and Sinks. 1990-2017. United States Environmental Protection Agency. EPA 430-R-19-001. 2019.Pdf.

(7) Karamian, E.; Sharifnia, S. On the General Mechanism of Photocatalytic Reduction of CO2. *J. CO2 Util.* **2016**, *16*, 194–203. https://doi.org/10.1016/j.jcou.2016.07.004.

(8) Johnson, M. P. Photosynthesis. *Essays Biochem.* **2016**, *60* (3), 255–273. https://doi.org/10.1042/EBC20160016.

(9) Wang, F.; Wang, W.-G.; Wang, H.-Y.; Si, G.; Tung, C.-H.; Wu, L.-Z. Artificial Photosynthetic Systems Based on [FeFe]-Hydrogenase Mimics: The Road to High Efficiency for Light-Driven Hydrogen Evolution. *ACS Catal.* **2012**, *2* (3), 407–416. https://doi.org/10.1021/cs200458b.

(10) Lodish, H.; Berk, A.; Zipursky, S. L.; Matsudaira, P.; Baltimore, D.; Darnell, J. Photosynthetic Stages and Light-Absorbing Pigments. *Mol. Cell Biol. 4th Ed.* **2000**.

(11) Rasheed, S. Photocatalytic Carbon Dioxide Reduction with Zinc(II) Dipyrrin Photosensitizers and Iron Catalyst. *Electron. Theses Diss.* **2020**, 66. https://dc.etsu.edu/etd/3730.

(12) Miessler, G. L.; Fischer, P. J.; Tarr, D. A. *Inorganic Chemistry*, Fifth edition.; Pearson: Boston, 2014.

(13) Hankache, J.; Niemi, M.; Lemmetyinen, H.; Wenger, O. S. Photoinduced Electron Transfer in Linear Triarylamine–Photosensitizer–Anthraquinone Triads with Ruthenium(II), Osmium(II), and Iridium(III). *Inorg. Chem.* **2012**, *51* (11), 6333–6344. https://doi.org/10.1021/ic300558s.

(14) Laine, P.; Campagna, S.; Loiseau, F. Conformationally Gated Photoinduced Processes within Photosensitizer–Acceptor Dyads Based on Ruthenium(II) and Osmium(II) Polypyridyl Complexes with an Appended Pyridinium Group. *Coord. Chem. Rev.* **2008**, *252* (23–24), 2552–2571. https://doi.org/10.1016/j.ccr.2008.05.007.

(15) Lakowicz, J. R.; Masters, B. R. *Principles of Fluorescence Spectroscopy*, 3rd ed.; Springer Science+Business Media, LLC: 233 Spring Street, New York, NY 10013, USA, 2006; Vol. 13.

(16) Trinh, C.; Kirlikovali, K.; Das, S.; Ener, M. E.; Gray, H. B.; Djurovich, P.; Bradforth, S. E.; Thompson, M. E. Symmetry-Breaking Charge Transfer of Visible Light Absorbing Systems: Zinc Dipyrrins. *J. Phys. Chem. C* **2014**, *118* (38), 21834–21845. https://doi.org/10.1021/jp506855t.

(17) Elbjeirami, O.; Rawashdeh-Omary, M. A.; Omary, M. A. Phosphorescence Sensitization via Heavy-Atom Effects in D10 Complexes. *Res. Chem. Intermed.* **2011**, *37* (7), 691. https://doi.org/10.1007/s11164-011-0342-7.

(18) Scharf, A. B. First-Row Transition Metal Complexes of Dipyrrinato Ligands: Synthesis and Characterization. Doctoral Dissertation. Harvard University. 2013.

(19) Filatov, M. A. Heavy-Atom-Free BODIPY Photosensitizers with Intersystem Crossing Mediated by Intramolecular Photoinduced Electron Transfer. *Org. Biomol. Chem.* **2020**, *18* (1), 10–27. https://doi.org/10.1039/C9OB02170A.

(20) van Willigen, H. Time-Resolved EPR Study of Photoexcited Triplet-State Formation in Electron-Donor-Substituted Acridinium Ions. *J. Phys. Chem.* **1996**, *100*, 3312–3316.

(21) Dance, Z. E. X.; Mi, Q.; McCamant, D. W.; Ahrens, M. J.; Ratner, M. A.; Wasielewski, M. R. Time-Resolved EPR Studies of Photogenerated Radical Ion Pairs Separated by *p* -Phenylene Oligomers and of Triplet States Resulting from Charge Recombination †. *J. Phys. Chem. B* **2006**, *110* (50), 25163–25173. https://doi.org/10.1021/jp063690n.

(22) Filatov, M. A.; Karuthedath, S.; Polestshuk, P. M.; Savoie, H.; Flanagan, K. J.; Sy, C.; Sitte, E.; Telitchko, M.; Laquai, F.; Boyle, R. W.; Senge, M. O. Generation of Triplet Excited States via Photoinduced Electron Transfer in *Meso* -Anthra-BODIPY: Fluorogenic Response toward Singlet Oxygen in Solution and in Vitro. *J. Am. Chem. Soc.* **2017**, *139* (18), 6282–6285. https://doi.org/10.1021/jacs.7b00551.

(23) Grabowski, Z. R.; Rotkiewicz, K.; Rettig, W. Structural Changes Accompanying Intramolecular Electron Transfer: Focus on Twisted Intramolecular Charge-Transfer States and Structures. *Chem. Rev.* **2003**, *103* (10), 3899–4032. https://doi.org/10.1021/cr940745l.

(24) Wood, T. E.; Thompson, A. Advances in the Chemistry of Dipyrrins and Their Complexes. *Chem. Rev.* **2007**, *107* (5), 1831–1861. https://doi.org/10.1021/cr050052c.

(25) Nyman, E. S.; Hynninen, P. H. Research Advances in the Use of Tetrapyrrolic Photosensitizers for Photodynamic Therapy. *J. Photochem. Photobiol. B* **2004**, *73* (1–2), 1–28. https://doi.org/10.1016/j.jphotobiol.2003.10.002.

(26) Kowada, T.; Maeda, H.; Kikuchi, K. BODIPY-Based Probes for Fluorescence Imaging of Biomolecules in Living Cells. *Chem. Soc. Rev.* **2012**, 21.

(27) Kçgel, J. F.; Kusaka, S.; Sakamoto, R.; Iwashima, T.; Tsuchiya, M.; Toyoda, R.; Matsuoka, R.; Tsukamoto, T.; Yuasa, J.; Kitagawa, Y.; Kawai, T.; Nishihara, H. Heteroleptic [Bis(Oxazoline)](Dipyrrinato)Zinc(II) Complexes: Bright and Circularly Polarized Luminescence from an Originally Achiral Dipyrrinato Ligand. *Angew Chem Int Ed* **2016**, 6.

(28) Lee, J.-S.; Kang, N.; Kim, Y. K.; Samanta, A.; Feng, S.; Kim, H. K.; Vendrell, M.; Park, J. H.; Chang, Y.-T. Synthesis of a BODIPY Library and Its Application to the Development of Live Cell Glucagon Imaging Probe. *J. Am. Chem. Soc.* **2009**, *131* (29), 10077–10082. https://doi.org/10.1021/ja9011657.

(29) Yogo, T.; Urano, Y.; Ishitsuka, Y.; Maniwa, F.; Nagano, T. Highly Efficient and Photostable Photosensitizer Based on BODIPY Chromophore. *J. Am. Chem. Soc.* **2005**, *127* (35), 12162–12163. https://doi.org/10.1021/ja0528533.

(30) Loudet, A.; Burgess, K. BODIPY Dyes and Their Derivatives: Syntheses and Spectroscopic Properties. *Chem. Rev.* **2007**, *107* (11), 4891–4932. https://doi.org/10.1021/cr078381n.

(31) Ulrich, G.; Ziessel, R.; Harriman, A. The Chemistry of Fluorescent Bodipy Dyes: Versatility Unsurpassed. *Angew. Chem. Int. Ed.* **2008**, *47* (7), 1184–1201. https://doi.org/10.1002/anie.200702070.

(32) Schmitt, A.; Hinkeldey, B.; Wild, M.; Jung, G. Synthesis of the Core Compound of the BODIPY Dye Class: 4,4′-Difluoro-4-Bora-(3a,4a)-Diaza-s-Indacene. *J. Fluoresc.* **2009**, *19* (4), 755–758. https://doi.org/10.1007/s10895-008-0446-7.

(33) Dudina, N. A.; Antina, E. V.; Nikonova, A. Yu.; Berezin, M. B.; Guseva, G. B.; V'yugin, A. I. Preparation and Spectral Properties of Zn(II) Complexes with Aryl-Substituted Dipyrrolylmethene and Azadipyrrolylmethene. *Russ. J. Gen. Chem.* **2013**, *83* (10), 1941–1943. https://doi.org/10.1134/S107036321310023X.

(34) Sazanovich, I. V.; Kirmaier, C.; Hindin, E.; Yu, L.; Bocian, D. F.; Lindsey, J. S.; Holten, D. Structural Control of the Excited-State Dynamics of Bis(Dipyrrinato)Zinc Complexes: Self-Assembling Chromophores for Light-Harvesting Architectures. *J. Am. Chem. Soc.* **2004**, *126* (9), 2664–2665. https://doi.org/10.1021/ja038763k.

(35) Trinh, C.; Kirlikovali, K.; Das, S.; Ener, M. E.; Gray, H. B.; Djurovich, P.; Bradforth, E.; Thompson, M. E. Symmetry Breaking Charge Transfer of Visible Light Absorbing System. 52.

(36) Kusaka, S.; Sakamoto, R.; Kitagawa, Y.; Okumura, M.; Nishihara, H. An Extremely Bright Heteroleptic Bis(Dipyrrinato)Zinc(II) Complex. *Chem. - Asian J.* **2012**, *7* (5), 907–910. https://doi.org/10.1002/asia.201200131.

(37) Kobayashi, A.; Hasegawa, T.; Yoshida, M.; Kato, M. Environmentally Friendly Mechanochemical Syntheses and Conversions of Highly Luminescent Cu(I) Dinuclear

Complexes. *Inorg. Chem.* **2016**, *55* (5), 1978–1985. https://doi.org/10.1021/acs.inorgchem.5b02160.

(38) Tungulin, D.; Leier, J.; Carter, A. B.; Powell, A. K.; Albuquerque, R. Q.; Unterreiner, A. N.; Bizzarri, C. Chasing BODIPY: Enhancement of Luminescence in Homoleptic Bis(Dipyrrinato) Zn ^{II} Complexes Utilizing Symmetric and Unsymmetrical Dipyrrins. *Chem. – Eur. J.* **2019**, *25* (15), 3816–3827. https://doi.org/10.1002/chem.201806330.

(39) Alqahtani, N. Z.; Blevins, T. G.; McCusker, C. E. Quantifying Triplet State Formation in Zinc Dipyrrin Complexes. *J. Phys. Chem. A* **2019**, *123* (46), 10011–10018. https://doi.org/10.1021/acs.jpca.9b08682.

(40) Tao, J.; Sun, D.; Sun, L.; Li, Z.; Fu, B.; Liu, J.; Zhang, L.; Wang, S.; Fang, Y.; Xu, H. Tuning the Photo-Physical Properties of BODIPY Dyes: Effects of 1, 3, 5, 7- Substitution on Their Optical and Electrochemical Behaviours. *Dyes Pigments* **2019**, *168*, 166–174. https://doi.org/10.1016/j.dyepig.2019.04.054.

(41) Suzuki, K.; Kobayashi, A.; Kaneko, S.; Takehira, K.; Yoshihara, T.; Ishida, H.; Shiina, Y.; Oishi, S.; Tobita, S. Reevaluation of Absolute Luminescence Quantum Yields of Standard Solutions Using a Spectrometer with an Integrating Sphere and a Back-Thinned CCD Detector. *Phys. Chem. Chem. Phys.* **2009**, *11* (42), 9850. https://doi.org/10.1039/b912178a.

(42) Crosby, G. A.; Demas, J. N. Measurement of Photoluminescence Quantum Yields. Review. *J. Phys. Chem.* **1971**, *75* (8), 991–1024. https://doi.org/10.1021/j100678a001.

(43) Méallet-Renault, R.; Pansu, R.; Amigoni-Gerbier, S.; Larpent, C. Metal-Chelating Nanoparticles as Selective Fluorescent Sensor for Cu $^{2+}$. *Chem Commun* **2004**, No. 20, 2344–2345. https://doi.org/10.1039/B407766K.

(44) González-Arjona, D.; López-Pérez, G.; Domínguez, M. M.; González, A. G. Solvatochromism: A Comprehensive Project for the Final Year Undergraduate Chemistry Laboratory. *J. Lab. Chem. Educ.* **2016**, *4* (3), 45–52. DOI: 10.5923/j.jlce.20160403.01.

(45) Reichardt, C. Solvatochromic Dyes as Solvent Polarity Indicators. *Chem. Rev.* **1994**, *94* (8), 2319–2358. https://doi.org/10.1021/cr00032a005.

(46) Williams, R. M. Introduction to Electron Transfer. **2007**. https://doi.org/10.13140/RG.2.2.16547.30244.

VITA

IRENE YAYRA DZAYE

Education:	M.S. Chemistry, East Tennessee State University, Johnson City, Tennessee, 2021
	B.Sc. Chemistry, Kwame Nkrumah University of Science and Technology, Kumasi, Ghana, 2017
Professional Experience:	Graduate Assistant, East Tennessee State University, College of Arts and Sciences, 2019-2021
	Teaching/Research Assistant, Kwame Nkrumah University of Science and Technology, Kumasi, Ghana, 2017-2018
Publications:	Mercy Badu, Mary-Magdalene Pedavoah & **Irene Yayra Dzaye** (2020): Proximate Composition, Antioxidant Properties, Mineral Content, and Anti-nutritional Composition of *Sesamum indicum*, *Cucumeropsis edulis* and *Cucurbita pepo* Seeds Grown in the Savanna Regions of Ghana, Journal of Herbs, spices & Medicinal Plants, DOI:10.1080/10496475.2020.1747581
Honors and Awards:	Second Class (Upper Division) Honors in B.Sc. Chemistry